# Plasma Levels of TMAO can be Increased with 'Healthy' and 'Unhealthy' Diets and Do Not Correlate with the Extent of Atherosclerosis but with Plaque Instability

Yen Chin Koay, PhD[#1,2,3], Yung-Chih Chen, DVM, PhD[#4], Jibran A. Wali, PhD[2,5], Alison W. S. Luk, BSc (Hons)[2,5], Mengbo Li, MPhil[2,6], Hemavarni Doma, BSc (Hons)[4], Rosa Reimark[4], Maria T.K. Zaldivia, PhD[4], Habteab T. Habtom, PhD[7,8], Ashley E. Frank, PhD[7,8], Gabrielle Fusco-Allison, BSc[1,2,3], Jean Yang, PhD[2,6], Andrew Holmes, PhD[2,5], Stephen J. Simpson, PhD[2,5], Karlheinz Peter, MD, PhD[4,#,*], John F. O'Sullivan, MD, PhD[1,2,3,9,#,*]

**Affiliations:**

[1]Heart Research Institute, The University of Sydney, New South Wales, Australia.

[2]Charles Perkins Centre, The University of Sydney, New South Wales, Australia.

[3]Central Clinical School, Sydney Medical School, Faculty of Medicine and Health, The University of Sydney, New South Wales, Australia.

[4]Baker Heart & Diabetes Institute, Melbourne, Victoria, Australia.

[5]Faculty of Science, School of Life and Environmental Sciences, The University of Sydney, New South Wales, Australia.

[6]School of Mathematics and Statistics, The University of Sydney, New South Wales, Australia.

[7]Department of Physiology, Anatomy and Microbiology, La Trobe University, Melbourne, Victoria, Australia.

[8]Centre for Future Landscapes, La Trobe University, Melbourne, Victoria, Australia.

[9]Department of Cardiology, Royal Prince Alfred Hospital, New South Wales, Australia.

[#]Equal authorship contributions

*Corresponding authors

**ABSTRACT**

Aims: The microbiome-derived metabolite trimethylamine-N-oxide (TMAO) has attracted major interest and controversy both as a diagnostic biomarker and therapeutic target in atherothrombosis.

Methods and Results: Plasma TMAO increased in mice on 'unhealthy' high-choline diets and notably also on 'healthy' high-fibre diets. Interestingly, TMAO was found to be generated by direct oxidation in the gut in addition to oxidation by hepatic flavin-monooxygenases. Unexpectedly, two well-accepted mouse models of atherosclerosis, ApoE$^{-/-}$ and Ldlr$^{-/-}$ mice, which reflect the development of stable atherosclerosis, showed no association of TMAO with the extent of atherosclerosis. This finding was validated in the Framingham Heart Study showing no correlation between plasma TMAO and coronary artery calcium score or carotid intima-media thickness, as measures of atherosclerosis in human subjects. However, in the tandem-stenosis mouse model, which reflects plaque instability as typically seen in patients, TMAO levels correlated with several characteristics of plaque instability, such as markers of inflammation, platelet activation, and intraplaque haemorrhage.

Conclusions: Dietary-induced changes in the microbiome, of both 'healthy' and 'unhealthy' diets, can cause an increase in the plasma level of TMAO. The gut itself is a site of significant oxidative production of TMAO. Most importantly, our findings reconcile contradictory data on TMAO. There was no direct association of plasma TMAO and the extent of atherosclerosis, both in mice and humans. However, using a mouse model of plaque instability we demonstrated an association of TMAO plasma levels with atherosclerotic plaque instability. The latter confirms TMAO as being a marker of cardiovascular risk.

Keywords: TMAO, bacterial microbiome, atherosclerosis, unstable plaque

**TRANSLATIONAL PERSPECTIVE**

There has been keen interest lately in the microbiome as a novel therapeutic target in the prevention and treatment of cardiovascular diseases. Trimethylamine-N-oxide (TMAO) is a microbiome-derived metabolite that has received a lot of interest as a novel biomarker and potential therapeutic target in atherothrombosis. However, there have been conflicting reports of its association with atherosclerosis and thrombosis, with some even showing an inverse association. In spite of this, in the correct context TMAO appears to be an excellent biomarker of subclinical atherosclerosis that can identify those at short-term and long-term risk of myocardial infarction. Herein, we reveal different dietary-microbiome interactions that help explain the apparent contradictions of TMAO's association with atherothrombosis. This insight is critical for the appropriate use of TMAO as a potential diagnostic and therapeutic target. Furthermore, using a unique murine model, we reveal TMAO to be associated with several features of plaque instability, providing insight into its utility as a marker of cardiovascular risk.

## INTRODUCTION

Gut microbial-derived metabolites have attracted major interest as biomarkers and mediators of disease.[1, 2] The metabolite trimethylamine-N-oxide (TMAO), in particular, has received a lot of attention as a novel marker of cardiovascular disease (CVD) and mediator of atherosclerosis and increased platelet activation.[3-6] It is proposed that increased dietary consumption of red meat or egg increases levels of nutrients such as choline, lecithin, and carnitine that are converted by gut bacteria to trimethylamine (TMA), which is oxidized by flavin-containing monooxygenases (FMOs), primarily in the liver, to TMAO,[7] which then exerts pro-atherogenic and platelet activation effects in the vasculature.[3-6]

Choline-supplemented chow increased atherosclerosis and macrophage lipid content in mice.[3] Furthermore, it was shown both *in vitro* and *in vivo* that TMAO increases platelet reactivity.[6] Efforts to translate these findings are quite mature, with companies offering plasma TMAO measurement in individuals as a means of determining cardiovascular risk, and development of approaches to inhibit TMA production in the gut as a means of treating atherosclerosis.[8] Yet, despite accumulating evidence of the association of TMAO with CVD events, its role in atherosclerosis remains controversial. Several reports did not support a correlation between TMAO and extent of atherosclerosis,[9-13] one in fact showing an inverse correlation between plasma TMAO level and atherothrombosis.[9] Likewise, in a population-based study in Norway, serum TMAO did not differ between patients with carotid atherosclerosis and healthy controls.[14] Two recent publications addressing the effect of dietary choline in the two most commonly used mouse models of atherosclerosis -- apolipoprotein E knockout ($ApoE^{-/-}$) mice[13] and both $ApoE^{-/-}$ and low-density lipoprotein receptor knockout ($Ldlr^{-/-}$) mice[12] -- concluded that atherosclerosis lesion size was not altered by a choline supplemented diet. Intriguingly, it was recently shown that TMAO administration in hypertensive rats had beneficial effects, significantly decreasing plasma

$NH_2$-terminal pro-B-type natriuretic peptide and vasopressin, left ventricular end diastolic pressure, and cardiac fibrosis.[15]

Notably, plasma TMAO increases after apparently healthy dietary interventions.[16, 17] It has been shown that plasma TMAO is actually increased more by fish and vegetable diets, reported as cardioprotective, than by red meat and egg diets considered to increase cardiovascular risk.[18] Other studies have shown that high-fibre diets in humans led to increased plasma TMAO,[19] however the underlying mechanism was unclear.

Therefore, in order to assess the relationship of TMAO to dietary context, and whether TMAO was related to atherosclerosis and cardiovascular risk, we examined divergent routes of TMAO generation in an 'unhealthy' (choline supplementation) and 'healthy' (high dietary fibre) dietary context, and explored its relationship to atherosclerosis in three different mouse models. We examined stable atherosclerosis using the most commonly used models of atherosclerosis: atherosclerosis-prone $ApoE^{-/-}$ and $Ldlr^{-/-}$ mice, and a tandem-stenosis model of plaque instability in $ApoE^{-/-}$ mice (see Supplementary Figure 1). The aims of this study were: (1) to evaluate the effect of 'unhealthy' (high choline) and 'healthy' (high fibre) diets on plasma TMAO levels and describe the different generative pathways in each case; (2) to examine the relationship between circulating TMAO levels and atherosclerosis in model systems and humans; (3) to characterize the relationship of TMAO and related metabolites to unstable plaque, the mechanism underlying cardiovascular events such as myocardial infarction. To address these specific aims, our sequence of experiments was: (1) Administer high-choline and high-fibre diets to mice and examine the effects on microbiome, faecal/plasma metabolite changes, and TMA oxidation enzyme expression; (2) In atherosclerosis-prone mice, examine the effect of choline supplementation on atherosclerosis, gut microbiome, and metabolites relevant to TMAO generation; (3) In parallel, examine the relationship of plasma TMAO to atherosclerosis in a well-characterized

human cohort; and (4) In a tandem-stenosis mouse model, representing plaque instability, examine the effect of choline supplementation on plaque instability and its relationship to TMAO and related metabolites.

# METHODS

## Mice and diets

Animal care and study protocols were approved by the institutional animal ethics committee at the University of Sydney (Protocol No. 2015/881) and the Alfred Research Alliance Animal Ethics committee (Protocol No. E/1721/2017/B), and all procedures conformed to the guidelines from Directive 2010/63/EU of the European Parliament on the protection of animals used for scientific purposes or the NIH Guide for the Care and Use of Laboratory Animals.

## High-fibre diet mice

C57BL/6J male mice (4 weeks old) for the dietary fibre study were purchased from Animal Resources Centre (Western Australia) and were housed four per cage (five cages per diet, n = 20 mice/diet, 6 of which were used for metabolomics). Commencing at 8 weeks of age, mice were fed *ad libitum* with one of two isocaloric low protein-high carbohydrate diets (14 kJ/g) containing 10% energy from protein, 70% from carbohydrate and 20% from fat (Specialty Feeds, Western Australia) for 18 weeks. The diets were kept isocaloric (14 kJ/g) with adjusted cellulose content. The diets were variations of the AIN93G standard semi-pure rodent diets (AIN93G provides ~19% of energy from protein, 17% from fat and 64% from carbohydrates).[20] Within the carbohydrate component, 35% energy was from sucrose and the remaining 65% from either native wheat starch or 'gel-crisp' high amylose resistant starch type-2 (CRISP FILM$^{TM}$ Starch from Ingredion, IL, USA).[21] Detailed compositions of the diets are listed in Supplementary Table 1. Mice were euthanized using overdose intraperitoneal injections of pentobarbital (Nembutal®, Abbott Laboratories, North Chicago, IL, USA; 25 mg/mL, 75 mg/kg) as approved by the Institutional Animal Ethics Committee at the University of Sydney.

**Atherosclerosis in ApoE$^{-/-}$ and Ldlr$^{-/-}$ mice**

Twenty-four male ApoE$^{-/-}$ and twenty-four Ldlr$^{-/-}$ mice obtained originally from the Animal Resource Centre in Western Australia, were bred in the Alfred Research Alliance animal facility. 6-week-old mice were fed a high-fat, high-cholesterol diet containing 22% fat and 0.15% cholesterol (SF00-219, Specialty Feeds, Western Australia) for 6 weeks. At 12 weeks of age, mice were provided high-choline, high-fat, high-cholesterol (SF17-200, 3% Choline, n = 12, Specialty Feeds) or low-choline, high-fat, high-cholesterol (SF00-219, 0.3% Choline, n = 12, Specialty Feeds) diets *ad libitum* until the end point. Mice were euthanized using overdose of 75 mg/kg intraperitoneal pentobarbital (Nembutal®, Abbott Laboratories, North Chicago, IL, USA). Detailed compositions of the diets are listed in Supplementary Table 2.

**Tandem stenosis (T/S) surgery in ApoE$^{-/-}$ mice**

This surgery has been previously described.[22] In short, male 6-week-old ApoE$^{-/-}$mice were fed HFD for 6 weeks. At 12 weeks of age, mice were anaesthetized by a ketamine (100mg/kg) and xylazine (10mg/kg) mixture through IP injection. An incision was made in the neck and the right common carotid artery was dissected from circumferential connective tissues. A T/S with 150 μm outer diameters was introduced with the distal point 1 mm from the carotid artery bifurcation and the proximal point 3 mm from the distal stenosis, stenosis diameter maintained with 150 μm sutured needle that was later removed. Animals were euthanized using overdose of 75 mg/kg intraperitoneal pentobarbital (Nembutal®, Abbott Laboratories, North Chicago, IL, USA) at 19 weeks of age.

**Quantification of atherosclerosis**

Frozen aortic sinuses were sectioned at 6 μm thickness for serial transverse sections, processed and stained as previously described.[23] At least 6 samples per mouse at 100 μm intervals were used. In the T/S mode, serial cryosections were obtained at 100 μm intervals at

1,500-2,000 µm proximal to the proximal suture in the right common carotid artery and from the brachiocephalic trunk and stored at -80°C until staining was performed. All histological analyses were performed by an operator blinded to animal treatment.

**Immunohistochemistry**

The left and right common carotid arteries and the brachiocephalic trunk were sectioned as described above. Sections were incubated in primary antibody [rabbit anti-mouse VCAM-1 (Santa Cruz sc-1504R, TX, USA) 1:200; rat anti-mouse TER-119 biotin (eBioscience 13-5921, CA, USA) 1:400; anti-smooth muscle actin antibody (ProteinTech 23081-1-AP, IL, USA) 1:200; and rat anti-mouse CD68 (Biorad MCA 1957, CA, USA) 1:200] at 4°C overnight, as described previously.

**Blood lipid analysis**

Total plasma cholesterol, LDL- and HDL-cholesterol, and triglyceride concentrations were measured as described previously.[22]

**Flow cytometry**

Mouse blood was collected by cardiac puncture using the anticoagulant heparin (20 IU/ml). Blood was then centrifuged at low speed (250 × g for 5 min using a soft break on a tabletop centrifuge) to remove red blood cells. Platelet-rich plasma (PRP) was obtained and diluted 1:50 in Phosphate-Buffered Saline (PBS) with 2 mM $Ca^{2+}$ and $Mg^{2+}$. The diluted PRP was stained for 15 min in the dark with anti-CD41 (APC, BD Biosciences) and anti-CD62P (PerCp, BD Biosciences). After incubation, Cell fix (BD Biosciences) was added. All samples were analyzed on a FACSCanto II flow cytometer (BD Bioscience). CD41-positive events were identified as platelets and platelet activation was defined by P-selectin expression.

**Sysmex haematology analysis**

Mouse blood was diluted at 1:7 in Cellpack (Biolab Diagnostics) for final total volume 100 $\mu$ L. The diluted blood samples were then mixed and run on the Sysmex (XS-1000i/XS-800i, Wakinohama-Kaigandori Chuo-ku, JAPAN) in Capillary mode, complete blood count (CBC) and differential measurements including: white blood cell count; red blood cell count; haemoglobin; haematocrit; mean corpuscular volume; mean corpuscular haemoglobin; mean corpuscular haemoglobin concentration; neutrophil count; lymphocyte count; monocyte count; eosinophil count; basophil count; nucleated red blood cell count; red blood cell distribution width standard deviation; red blood cell distribution width coefficient of variation; mean platelet volume; reticulocyte count; and immature reticulocyte fraction data were collected.

**Metabolomics**

Blood was collected immediately by cardiac puncture using heparinized syringes and sample tubes, then centrifuged to isolate plasma. Aliquots of plasma were frozen on dry ice and stored at -80 °C until analysis. Faecal samples upon collection were freeze-dried immediately and stored at -80 °C until analysis.

Targeted metabolomic analysis measured hydrophilic metabolites in both positive and negative ionization mode using an LC-MS/MS system comprised of an Agilent 1260 Infinity liquid chromatography (LC) system coupled to a QTRAP 5500 mass spectrometer (MS) (AB SCIEX), as previously described.[21]

**Quantification of metabolites**

Quantification using calibration curves based on the standard-addition method was used to eliminate matrix effects and for quantitative analysis of choline, betaine, L-carnitine, TMA, TMAO, CA, and DCA in plasma and faecal samples, as previously described.[24] Briefly, pooled plasma and faeces extracts were divided into aliquots of equal volumes and

were spiked with known and varying amounts of the analytes of interest to build the calibration curve. The calibration curves showed a very good correlation between concentration and response, R-squared for all calibrants was greater than 0.995 Absolute concentrations of each metabolite in the pooled plasma and faeces are reported in Supplementary Table 3.

**qRT-PCR**

10 mg of liver tissues was homogenized in Trizol (Life technologies). Total RNA was isolated using 1-bromo 3-chloropropane for phase separation for total RNA precipitation according to published protocol.[25] RNA was quantified spectrophotometrically using a NanoDrop (Thermo Scientific). cDNA was synthesized (BioRad iScript) and real-time PCR was performed using TaqMan® Gene Expression Assays (Life Technologies) to measure *HMGCR* (4331182; MM012824990_m1), *CYP7A1* (4331182; MM00484150_m1), *FMO1* (4331182; MM00515795_m1), *FMO2* (4331182; MM00490159_m1), *FMO3* (4331182; MM01306345_m1) and *NR1H4/FXR* (4331182; MM00436425_m1) according to manufacturer's instructions. Reactions were performed in triplicate and target gene expression was normalized to the house keeping gene *GAPDH* (4331182; MM99999915_g1) and analyzed using the ΔΔCt method.

**Bacterial microbiome analysis**

In the dietary fibre study, total DNA was extracted from caecal samples and the bacterial community was profiled using the 16S rRNA V4 region as previously described.[21] In the choline study, total DNA was extracted from faecal samples using QIAamp ® Fast DNA Stool Mini Kit (QIAGEN, catalog number: 51604), and the bacterial community was profiled using the 16S rRNA V1-V3 (27F-519 R) andV3-V4 region (341F – 806R). Sequencing was performed Illumina MiSeq.

For each study, sequence analysis was performed in R v3.5.1.[26] Sequence reads were aligned and partitioned into amplicon sequence variants (ASVs) using DADA2 v1.10.1.[27] Taxonomy was assigned to ASVs against the SILVA database v128.[28] Multiple sequence alignment was performed with the msa package v.1.14.0,[29] phylogenetic tree construction was performed with the phangorn package v.2.5.3[28] and rooted using the ape package v.5.2.[30] ASVs that contained less than 0.01% of total reads or less than 0.1% of reads in at least two samples were filtered out. After filtering, the minimum reads per sample was 14,799 for the choline study and 39,306 for the dietary fibre study. Principal coordinate analysis ordination of weighted UniFrac distances[31] of gut microbial communities was performed using the phyloseq package v.1.26.1[32] and visualized with ggplot2 package v.3.1.0.[33]

The raw sequence reads for the RS vs NS study are available at the National Center for Biotechnology Information (NCBI) Sequence Read Archive in BioProject PRJNA531040, under the accession numbers SRR8859087, SRR8859088, SRR8859091-SRR8859093, SRR8859099, SRR8859103, SRR8859106 and SRR8859109 and the raw sequence reads for the choline study are available under the accession numbers SRR10961733-10961756.

**Framingham heart study offspring cohort**

For participants from the Offspring cohort who attended Exam 5 in the Framingham Heart Study, LC-MS/MS metabolomic profiling was performed on plasma specimens collected from each individual. The concentration of plasma metabolites was normalised to pooled plasma samples, followed by a $\log_2$ transformation and centralisation to the median. Carotid intima-media thickness (IMT) measurements were obtained for subjects attending Exam 6, and coronary artery calcium scores (CAS) for those who attended Exam 7. To examine associations of TMAO with CAS and IMT, linear models stratified by age were fitted for $\log_{100}(\text{CAS} + 1)$ (with non-zero CAS only) and log-transformed IMT to account for right-skewed distributions. Analyses were performed with the *lm* function in R (3.5.2).

**Statistical analyses**

Data are expressed as the mean ± SEM and were compared using Student's t-test, with *P* values <0.05 considered statistically significant. Correlation of microbial abundance against metabolites was performed separately for the dietary fibre study and the choline study in R v3.5.1.[26] Microbial abundance data was centre-log ratio transformed with the compositions package v.1.40.2[34] and partial least squares regression was performed with the plsdepot package v.0.1.17.[35] Analysis of variance based on weighted UniFrac distances between microbial communities was performed with the vegan package v.2.5.4.[36]

## RESULTS

### *Choline-driven changes*

To investigate atherosclerotic plaque progression, we used the two most common animal models of atherosclerosis. ApoE$^{-/-}$ and Ldlr$^{-/-}$ mice were studied at two time points: at 6 weeks of age, mice were given high fat diet for 6 weeks. At 12 weeks of age, mice were randomly assigned to high-choline (3%) vs low-choline (0.3%) high-fat, high-cholesterol diets for a further 7 weeks in ApoE$^{-/-}$ mice and for a further 14 weeks in Ldlr$^{-/-}$ mice. The durations of study diets were chosen according to the reported temporal development of atherosclerosis in each of these atherosclerosis-prone strains, with Ldlr$^{-/-}$ mice typically needing longer for atherosclerosis development as ApoE$^{-/-}$ mice.[37, 38] Several TMAO-related metabolites were significantly changed by choline supplementation. High-choline diets resulted in significant increases in plasma choline in both ApoE$^{-/-}$ (fold change (FC) = 1.8, P = 7.8x10$^{-3}$) and Ldlr$^{-/-}$ mice (FC = 1.4, P = 2x10$^{-2}$) (Fig. 1A). Betaine, oxidative product of choline, was significantly elevated in ApoE$^{-/-}$ (FC = 1.3, P = 1.9x10$^{-3}$) and Ldlr$^{-/-}$ mice (FC = 1.1, P = 6.0x10$^{-3}$), consistent with previous reports revealing choline conversion to TMA via betaine (trimethylglycine).[39] High-choline diets did not cause differences in carnitine levels in either strain (Fig 1A).

TMA and TMAO were dramatically increased in the plasma. Plasma levels of TMA in ApoE$^{-/-}$ (FC = 18.4, P = 6x10$^{-5}$) and Ldlr$^{-/-}$ (FC = 3.8, P = 9x10$^{-4}$); and TMAO in ApoE$^{-/-}$ (FC = 8.9, P = 2x10$^{-9}$) and Ldlr$^{-/-}$ (FC = 2.9, P = 3.5x10$^{-5}$) mice (Fig. 1B), significantly increased.

Bile acids can induce expression of FMOs, the enzyme that oxidizes TMA to TMAO, *via* their cognate receptor farnesoid X-receptor (FXR). Choline supplementation did not change bile acid concentrations. There were no significant changes in plasma primary bile acid (cholic acid) or secondary bile acid (deoxycholic acid) in either strain (Fig. 1C). The

enzymes that oxidize TMA to TMAO, FMOs, decreased or did not change. In the $Ldlr^{-/-}$ mice fed high-choline diets for 14 weeks, hepatic expression of FMO3 (FC = 0.35, P = $4x10^{-3}$) significantly decreased, whereas FMO1 and FMO5 expression were non-significantly decreased (Fig. 1D).

***Fibre-driven changes***

Plasma and faecal samples from both native starch (NS)- and high-fibre resistant starch (RS)-fed mice were collected, processed, and subjected to metabolomic analysis according to established protocols with minor modifications.[21]

The C57BL/6J mouse strain is an often used animal model for the study of dietary interventions and we found that C57BL/6J mice after 18 weeks of high-RS feeding had significantly higher circulating levels of TMA (FC = 3.6, P = $5x10^{-3}$) (Fig. 2A) and TMAO (FC = 2.9, P = $4x10^{-4}$) (Fig. 2A). Faecal TMA levels were significantly higher (FC = 3.2, P = $3x10^{-3}$) (Fig. 2B) in RS-fed mice when compared to NS-fed mice. TMAO was readily detectable in the faeces, and levels were lower in the faeces of RS mice *vs* NS mice (Fig. 2B), although not statistically significant (FC = 0.34, P = 0.06). Mean absolute plasma and faecal concentrations of TMAO were determined using quantitative analysis by the standard addition method to compare NS-fed and RS-fed mice (both pooled across 6 samples) (Supplementary Table 3). In NS mice, the plasma concentration of TMAO (0.5 µM) was similar to that in the faeces (0.2 µM); however, in RS mice, plasma TMAO was strikingly higher (6.2 µM) than faecal TMAO (0.07 µM). As faecal TMA was increased in RS mice, the dramatic reduction in faeces: plasma TMAO ratio suggests altered TMAO transport between the gut and the circulation.

Despite an increase in plasma TMA and TMAO levels in RS mice, plasma choline levels were significantly decreased in RS-fed mice (FC = 0.72, P = $7x10^{-3}$) (Fig. 2C). Faecal levels of choline were unchanged between the RS- and NS-fed mice (Fig. 2D). There were no

significant differences in plasma or faecal levels of betaine between RS- and NS-fed mice (Fig. 2C and 2D). Interestingly, L-carnitine, which is structurally similar to choline and can be synthesized from L-lysine and L-methionine, was significantly higher in the plasma of RS-fed mice (FC = 1.3, P = $1x10^{-2}$) (Fig. 2C), but had a trend towards decreased concentration in the faeces (FC = 0.39, P = 0.1) (Fig. 2D).

As mentioned above, bile acids are important inducers of expression of the FMO family of genes, which oxidize TMA to TMAO, and high-fibre diets caused increases in plasma bile acid concentrations. Plasma levels of the primary bile acid, cholic acid (CA), were significantly higher in RS-fed mice (FC = 6.6, P = $2x10^{-3}$) (Fig. 2E) but not different in the faeces (Fig. 2F). The microbial-derived secondary bile acid deoxycholic acid (DCA) significantly decreased (FC = 0.49, P = $2x10^{-2}$) (Fig. 2F) in the faeces of RS-fed mice, but significantly increased (FC = 6.2, P = $2x10^{-5}$) (Fig. 2E) in the plasma. Using plasma: faecal ratios based on absolute concentrations, on NS the plasma: faecal ratio of primary bile acid cholic acid was 0.28:1 and this increased on RS to 0.79:1. On NS, plasma: faecal ratio of secondary bile acid deoxycholic acid was 1:1, and on RS this ratio increased dramatically to 5.1:1. This pattern of decreased faecal concentration in concert with increased plasma concentration suggests increased reabsorption in the ileum, cycling through the enterohepatic circulation.

Mice fed on RS diet also showed a significant increase in hepatic expression of cholesterol 7α-hydroxylase (CYP7A1) (FC = 3.7, P = $4x10^{-2}$) (Fig. 2G), which catalyzes the formation of 7-α-hydroxycholesterol from cholesterol and is the rate-limiting step for the production of bile acids in the liver. This finding is consistent with our previous report showing significant reduction in plasma cholesterol in RS mice.[21] We also observed a significant increase in the hepatic expression of the rate-limiting enzyme for cholesterol synthesis, 3-hydroxy-3-methylglutaryl-coenzyme A reductase (HMGCR) in RS mice (FC =

2.4, P = $1x10^{-2}$) (Fig. 2G). On RS-fed mice, FXR (cognate hepatic bile acid receptor) and FMO1 expression did not change, but FMO2 (FC = 1.74, P = 0.046) expression was significantly increased whilst FMO3 expression was borderline significantly increased (FC = 2.94, P = 0.06) (Fig. 2H).

***Distinct microbiome-metabolite correlations***

Principal coordinate analysis of the bacterial gut microbiota indicated that dietary fibre drove greater bacterial changes than dietary choline (Fig. 3A and 3C, Supplementary Figure 2). The maximum variance explained in C57BL/6J mice fed RS vs NS diets was 77.7% (p = 0.009) compared to 35.3% (p = 0.002) in $ApoE^{-/-}$ mice fed high-choline vs low-choline diets.

For further analyses, metabolites with major changes upon dietary interventions were chosen. Distinct bacterial taxa were associated with TMA and TMAO levels in the two studies. In high-choline vs low-choline fed mice, partial least squares regression analysis indicated strong positive correlations between plasma choline, TMA, and TMAO levels with bacterial amplicon sequence variants (ASVs) assigned to the genera *Enterorhabdus* (R = 0.76-0.88) and *Lachnoclostridium* (R = 0.70-0.80) (Fig. 3B). In RS- vs NS-fed mice, the strongest positive correlations to faecal TMA and plasma TMA levels was with ASVs assigned to the order *Bacteroidales* (R = 0.79-0.84) and the genus *Allobaculum* (R = 0.79-0.84) (Fig. 3D). These ASVs showed a weaker positive correlation with plasma TMAO levels (R = 0.63-0.72) (Fig. 3D). No ASVs showed strong positive correlated with faecal TMAO levels (R < 0.50).

***High-choline diets did not alter atherosclerotic burden or plaque composition***

High-choline (3%) vs low-choline (0.3%) high-fat, high-cholesterol diets were administered in $ApoE^{-/-}$ and in $Ldlr^{-/-}$ mice as described in Methods. There was no significant change in atherosclerotic plaque burden in either $Ldlr^{-/-}$ (Fig. 4 A) or $ApoE^{-/-}$ (Fig. 4F) mice.

Plaque composition determines stability,[40] and we found no significant changes in plaque burden or histological features, including necrotic core (Fig. 4B+G), neutral lipids (Fig. 4C+H), macrophage content (CD68; Fig. 4D+I), or collagen (Fig. 4E+J) in 0.3% vs 3% choline high-fat, high-cholesterol diets in both Ldlr$^{-/-}$ and ApoE$^{-/-}$ murine strains.

***High-choline diets did not alter plasma lipids but increased circulating monocytes, neutrophils, and platelet activation***

We next investigated circulating plasma lipids and immune cells in high-choline treated mice. High-choline supplementation did not alter plasma triglycerides (Fig. 5A), cholesterol (Fig. 5B), high density lipoproteins (Fig. 5C), low density lipoproteins/very low density lipoproteins (Fig. 5D), lymphocytes (Fig. 5E, Sysmex) or any other parameter determined in Sysmex (see Methods), but did increase circulating levels of monocytes (Fig. 5F, Sysmex), neutrophils (Fig. 5G, Sysmex), and expression of P-selectin on the platelet surface (CD41$^{+}$ P-selectin$^{+}$) (Fig. 5H, flow cytometry), the latter indicating increased platelet activation.

It has been previously shown that endothelial dysfunction characterized by reduced bioavailability of nitric oxide (NO) contributes to platelet activation.[41, 42] We found that $N^{G}$,$N^{G}$-dimethyl-L-arginine (ADMA) (FC = 1.3, P = 0.009) and $N^{G}$-monomethyl-L-arginine (L-NMMA) (FC = 1.3, P = 0.01) (Fig. 5I) (both inhibitors of NO synthase) were significantly higher in the plasma of high choline-fed mice. Increased levels of ADMA and L-NMMA limit NO synthesis from L-arginine, which may contribute to platelet activation.

***High-choline diets increased intra-plaque haemorrhage in a mouse model of plaque instability***

We then investigated the effects of choline supplementation in a recently established mouse model of plaque instability, which is based on haemodynamic changes induced by a tandem-stenosis in the right carotid artery.[22] This model uniquely reflects plaque

instability/vulnerability as seen in patients and has been extensively validated histologically, in mRNA and miRNA expression profiling as well as by its use for imaging of unstable plaques and therapeutic plaque stabilisation.[22, 23, 43-45] In this mouse model, we found no changes in neutral lipids by oil red O (Fig. 6A), CD68 (Fig. 6B), VCAM-1 (Fig. 6C), smooth muscle alpha actin (Fig. 6D), platelet count by CD42c (Fig. 6E), and collagen (Fig. 6F) in 3% vs 0.3% choline high-fat, high-cholesterol diets. Nevertheless, our investigation of one of the most prominent plaque instability markers -- intraplaque haemorrhage[23, 46] -- indicated significantly increased plaque instability on high-choline supplementation as determined by increased ferritin (Perl's iron) and erythrocyte marker TER-119 (Fig. 6G, H).

***Plasma TMAO did not associate with atherosclerosis in the Framingham Heart Study***

Plasma TMAO was not associated with atherosclerosis, as defined by coronary artery calcium score (CAS) (Fig. 7a) and carotid intima-media thickness (IMT) (Fig. 7b) in the Framingham Heart Study Offspring cohort. Here, we performed logistic regression of CAS or carotid IMT with plasma TMAO levels in 628 and 587 individuals, respectively. We stratified analysis according to age and did not see a significant association across age groups. Grouping all individuals together, there remained no association (beta coefficient = 0.016, P = 0.45). In all age categories, there was no association between plasma TMAO levels and carotid IMT (Fig. 7b), and grouping all age ranges together, there remained no association (beta coefficient = 0.003, P = 0.94).

## DISCUSSION

Our data provide novel insights into the mechanisms underlying increased plasma TMAO levels in two divergent contexts. First, although we saw dramatic elevations of plasma TMA and TMAO, we didn't observe any change in atherosclerotic plaque burden and composition induced by 3% choline-supplemented vs 0.3% choline supplemented high-fat,

high-cholesterol diets in two atherosclerosis-prone mouse strains at 7 or 14 weeks of feeding. ApoE$^{-/-}$ mice on a Western diet develop aortic fatty streaks by 5 weeks and plaques by 7-8 weeks[38] and we saw no augmentation of this process using 3% compared to 0.3% choline supplementation. Similarly, Ldlr$^{-/-}$ mice on Western diets develop aortic plaques by 12 weeks[37], however, despite significantly-elevated TMA and TMAO in both strains, we did not see any change in atherosclerosis with 3% compared to 0.3% choline supplementation. TMAO levels were positively correlated with ASVs assigned to the bacteria genera *Enterorhabdus* and *Lachnoclostridium*. *Lachnoclostridium* is known to be involved in TMA synthesis from dietary choline by the action of choline TMA-lyase (CutC).[47]

TMA can be oxidized to TMAO *via* the action of gut bacterial enzymes or by hepatic enzyme FMO3.[48, 49] It is reported that almost all TMA is passively absorbed in the portal circulation and oxidized to TMAO in the liver[50], but our results suggest that this is dependent on dietary-microbiome context. In fact, we show that TMAO is readily detectable in the faeces at similar concentrations to the plasma. A significant decrease in hepatic expression of FMO3 accompanied by a significant increase in plasma levels of TMAO after 14 weeks of high-choline diet points towards the gut as the potential source of oxidation to TMAO. Notably, plasma TMAO levels of the mice fed on high-choline diet were highly positively correlated with the abundance of bacterial ASVs assigned to genus *Enterorhabdus*. Bacterial species within this genus are commonly observed in mouse models of inflammatory disease,[51-53] and their active mucin-degrading capabilities can lead to inadvertent penetration of commensal bacteria that may come in direct contact with the gut epithelium,[54] leading to elevated production of antimicrobial reactive oxygen species such as superoxide, hydrogen peroxide, and hydroxyl radical in the gut,[55] which can oxidize TMA to TMAO.[56, 57] Consistent with these findings, the ratio of glutathione (GSH), an important scavenger of reactive oxygen species[58] to the oxidized disulfide form of GSH (GSSG), a commonly used

marker of oxidative stress, was decreased at borderline significance in high-choline fed mice (FC = 2.4, P = 0.06), suggesting an increase in oxidative stress (Supplementary Figure 3).

There is a particular interest in the effects of high-fibre diets on the microbiome and consequent health benefits. Resistant starch (RS), a type of dietary fibre found in a wide variety of food, such as whole grains, legumes, cooked and chilled pasta, potatoes and rice, and unripe bananas is highly representative of the most common dietary fibres ingested by humans.[59] When mice were administered an RS diet, there was a strong increase in plasma bile acids and TMA compared to the NS-fed mice. Bile acids are known inducers of the FMO family of genes in the liver *via* FXR, which oxidize TMA to TMAO, and FMOs were increased on RS diet. We have previously shown that RS-fed mice had significantly lower plasma cholesterol,[21] and lower plasma cholesterol accompanied by a marked increase in plasma bile acids suggests that dietary fibre may exert cholesterol-lowering effects through bile acid synthesis. Bile acids are predominantly synthesized from cholesterol *via* the neutral pathway involving CYP7A1,[60] which catalyses the formation of 7-α-hydroxycholesterol and is the rate-limiting step of bile acid synthesis.[60, 61] The increased expression of hepatic CYP7A1 in RS-fed mice indicates increased conversion of cholesterol to bile acids, as reported previously using oat bran in the same murine model.[62] Reduced liver cholesterol leads to the activation of HMGCR to increase cholesterol synthesis. High-fibre diets are known to increase metabolite absorption from the colon,[21] likely explaining the increase in TMA and secondary bile acids in this context. Although we did not observe a change in FXR at the mRNA level, it is well established that elevated circulating bile acids activate the nuclear hormone receptor FXR in the liver, which induces hepatic FMO3 expression to increase conversion of TMA to TMAO,[43] and we saw elevated hepatic FMO2 and FMO3 expression on RS diets. Furthermore, bacterial taxa showed stronger positive correlations to faecal and plasma TMA levels than TMAO levels. Together, these data suggest that high-

choline diets lead to oxidation of TMA to TMAO in the gut, but high-fibre diets convert cholesterol to bile acids, which activate hepatic FMOs that oxidize the increased TMA to generate TMAO in the liver.

Intriguingly, we did not see any changes in atherosclerotic burden or plaque composition induced by high-choline diets with elevated plasma TMAO. This is in contrast to earlier studies describing an association of TMAO plasma levels and atherosclerosis in mice.[3] However, more recent studies could not confirm this association and as such are consistent with our findings in mouse atherosclerosis.[9-11, 44] Furthermore, clinical association studies again initially described a positive correlation between cardiovascular risk and TMAO level, which was not confirmed in subsequent studies.[10, 45] Our investigation in the Framingham Heart Study did not reveal an association of TMAO with atherosclerosis.

There could be several reasons for these controversial results. In mice, these include differences in baseline bacterial gut microbiome between similar mouse strains from different vendors, diet (e.g. different choline levels), mouse age, animal housing conditions, and duration of experiments. In human studies these include differences in ethnicity and patient age; and gender, diet, and medication usage that can introduce a change in the gut bacterial microbiome composition and alter the relationship between TMAO and atherosclerosis. However, arguably the most important reason is that TMAO is but one of many factors that can influence atherosclerosis and its complications. Depending on the magnitude of each factor, TMAO could be more or less dominant. Although plasma TMAO was increased in mice on a high-choline diet, so were other metabolites with known associations to platelet activation and vascular inflammation such as ADMA[63, 64] and L-NMMA.[65] Overall, it is highly likely that, rather than a single mediator such as TMAO, high-choline diets exert their effects via a constellation of these pro-inflammatory and platelet-activating mediators.

Despite this, TMAO has been demonstrated to have clinical utility in predicting future cardiovascular events, independent of traditional risk factors and even in patients who are negative for troponin T[66] and this is consistent with our findings in the tandem-stenosis model, which recreates the histological features of plaque instability seen in humans.[23, 67-69] Histopathological analysis of plaque rupture and the increased circulating TMAO in multiple human clinical studies suggest a relationship of TMAO with plaque instability,[70-72] and these results were consistent with our mouse models of tandem stenosis, whereby high-choline diets led to greater intraplaque haemorrhage and platelet activation, two pathological features of unstable plaques. Although we found elevations in plasma levels of other relevant mediators such as ADMA and L-NMMA, these have not performed as well as TMAO as predictive biomarkers in terms of effect size and significance and have not been replicated in as large cohort sizes as has TMAO.[73, 74] Therefore, in the correct context, TMAO appears to be an excellent circulating biomarker of subclinical disease that manifests as atherothrombosis either in the short or long-term.[6, 66] As plaque instability cannot be studied in stable atherosclerosis models such as ApoE$^{-/-}$ and Ldlr$^{-/-}$, our model provides insight into the context underlying the predictive capability of TMAO for atherothrombotic risk.

## CONCLUSION

Our data reveal distinct dietary – bacterial microbiome interactions leading to elevated plasma TMAO, in both 'healthy' and 'unhealthy' dietary contexts and provide insight into the conflicting reports of TMAO's relationship to atherothrombosis. Our data suggest that there is no direct association of plasma TMAO and the extent of atherosclerosis. However, we did demonstrate an association of TMAO plasma levels with atherosclerotic plaque instability. The latter is in accordance with TMAO being associated with an increased risk of cardiovascular events.

## ACKNOWLEDGEMENTS

This work was supported by the Heart Research Institute (JOS & YCK), Sydney Medical School Foundation Chapman Fellowship (JOS), and by NSW Health Early-Mid Career Fellowship (JOS). KP was supported by a NHMRC Principle Research Fellowship. YCC was supported by a Future Leader Fellowship (Reference No.102068) from the National Heart Foundation of Australia. The Framingham Heart Study is conducted and supported by the National Heart, Lung, and Blood Institute (NHLBI) in collaboration with Boston University (Contract No. N01-HC-25195 and HHSN268201500001I). This manuscript was not prepared in collaboration with investigators of the Framingham Heart Study and does not necessarily reflect the opinions or views of the Framingham Heart Study, Boston University, or NHLBI. Funding for SHARe Affymetrix genotyping was provided by NHLBI Contract N02-HL-64278. SHARe Illumina genotyping was provided under an agreement between Illumina and Boston University. Funding for Affymetrix genotyping of the FHS Omni cohorts was provided by Intramural NHLBI funds from Andrew D. Johnson and Christopher J. O'Donnell. Funding support for the Framingham Targeted and Untargeted Metabolomics – HILIC – Installment 1 dataset was provided by Massachusetts General Hospital Departmental funding. Funding support for the Framingham Metabolomics (HILIC - Installment 1, 2 and 3) datasets, Framingham Central Metabolomics - HILIC – Installment 1 and 2, and Lipid Platform – Installment 1 and 2, were provided by NIH grant R01 DK081572.

## CONFLICTS OF INTEREST

All authors declare that they have no conflicts of interest.

## AUTHOR CONTRIBUTIONS

YCK performed, acquired and analysed all metabolomic data, performed qRT-PCR in the high-fibre livers, and wrote the manuscript. YCC performed the high choline mice experiments, including all atherosclerosis analysis and the tandem stenosis experiments. JAW performed the high-fibre diet murine experiments. AWSL performed the high-fibre microbiome experiments. MTKZ conducted and analyzed Sysmex and flow cytometry experiments. ML performed statistical analyses of the Framingham subjects. HD, RR, HTH, and AEF performed and analysed microbiome experiments in the high-choline diet mice. GFA performed qRT-PCR in the high-fibre livers. JY supervised all statistical analyses. AH supervised microbiome experiments in the high-fibre mice. SJS supervised high-fibre experiments and analysis, and wrote the manuscript. KP supervised the high-choline murine studies and wrote the manuscript. JOS supervised the high-fibre metabolic experiments and wrote the manuscript. KP and JOS conceived the study.

## REFERENCES


1. Tang WHW, Li DY, Hazen SL. Dietary metabolism, the gut microbiome, and heart failure. *Nat Rev Cardiol*. 2019;**16**:137-54.
2. Schroeder BO, Backhed F. Signals from the gut microbiota to distant organs in physiology and disease. *Nat Med*. 2016;**22**:1079-89.
3. Wang Z, Klipfell E, Bennett BJ, Koeth R, Levison BS, Dugar B, Feldstein AE, Britt EB, Fu X, Chung YM, Wu Y, Schauer P, Smith JD, Allayee H, Tang WH, DiDonato JA, Lusis AJ, Hazen SL. Gut flora metabolism of phosphatidylcholine promotes cardiovascular disease. *Nature*. 2011;**472**:57-63.
4. Koeth RA, Wang Z, Levison BS, Buffa JA, Org E, Sheehy BT, Britt EB, Fu X, Wu Y, Li L, Smith JD, DiDonato JA, Chen J, Li H, Wu GD, Lewis JD, Warrier M, Brown JM, Krauss RM, Tang WH, Bushman FD, Lusis AJ, Hazen SL. Intestinal microbiota metabolism of L-carnitine, a nutrient in red meat, promotes atherosclerosis. *Nat Med*. 2013;**19**:576-85.
5. Tang WH, Wang Z, Levison BS, Koeth RA, Britt EB, Fu X, Wu Y, Hazen SL. Intestinal microbial metabolism of phosphatidylcholine and cardiovascular risk. *N Engl J Med*. 2013;**368**:1575-84.
6. Zhu W, Gregory JC, Org E, Buffa JA, Gupta N, Wang Z, Li L, Fu X, Wu Y, Mehrabian M, Sartor RB, McIntyre TM, Silverstein RL, Tang WHW, DiDonato JA, Brown JM, Lusis AJ, Hazen SL. Gut Microbial Metabolite TMAO Enhances Platelet Hyperreactivity and Thrombosis Risk. *Cell*. 2016;**165**:111-24.
7. Wang Z, Klipfell E, Bennett BJ, Koeth R, Levison BS, DuGar B, Feldstein AE, Britt EB, Fu X, Chung Y-M. Gut flora metabolism of phosphatidylcholine promotes cardiovascular disease. *Nature*. 2011;**472**:57.
8. Wang Z, Roberts AB, Buffa JA, Levison BS, Zhu W, Org E, Gu X, Huang Y, Zamanian-Daryoush M, Culley MK, DiDonato AJ, Fu X, Hazen JE, Krajcik D, DiDonato JA, Lusis AJ, Hazen SL. Non-lethal Inhibition of Gut Microbial Trimethylamine Production for the Treatment of Atherosclerosis. *Cell*. 2015;**163**:1585-95.
9. Yin J, Liao SX, He Y, Wang S, Xia GH, Liu FT, Zhu JJ, You C, Chen Q, Zhou L, Pan SY, Zhou HW. Dysbiosis of Gut Microbiota With Reduced Trimethylamine-N-Oxide Level in Patients With Large-Artery Atherosclerotic Stroke or Transient Ischemic Attack. *J Am Heart Assoc*. 2015;**4**.
10. Meyer KA, Benton TZ, Bennett BJ, Jacobs DR, Jr., Lloyd-Jones DM, Gross MD, Carr JJ, Gordon-Larsen P, Zeisel SH. Microbiota-Dependent Metabolite Trimethylamine N-Oxide and Coronary Artery Calcium in the Coronary Artery Risk Development in Young Adults Study (CARDIA). *J Am Heart Assoc*. 2016;**5**.
11. Mueller DM, Allenspach M, Othman A, Saely CH, Muendlein A, Vonbank A, Drexel H, von Eckardstein A. Plasma levels of trimethylamine-N-oxide are confounded by impaired kidney function and poor metabolic control. *Atherosclerosis*. 2015;**243**:638-44.
12. Aldana-Hernández P, Leonard K-A, Zhao Y-Y, Curtis JM, Field CJ, Jacobs RL. Dietary Choline or Trimethylamine N-oxide Supplementation Does Not Influence Atherosclerosis Development in Ldlr−/− and Apoe−/− Male Mice. *J Nutr*. 2019.
13. Lindskog Jonsson A, Caesar R, Akrami R, Reinhardt C, Fåk Hållenius F, Borén J, Bäckhed F. Impact of gut microbiota and diet on the development of atherosclerosis in ApoE−/− mice. *Arterioscler Thromb Vasc Biol*. 2018;**38**:2318-26.
14. Skagen K, Trøseid M, Ueland T, Holm S, Abbas A, Gregersen I, Kummen M, Bjerkeli V, Reier-Nilsen F, Russell D. The Carnitine-butyrobetaine-trimethylamine-N-oxide pathway and its association with cardiovascular mortality in patients with carotid atherosclerosis. *Atherosclerosis*. 2016;**247**:64-9.

15. Huc T, Drapala A, Gawrys M, Konop M, Bielinska K, Zaorska E, Samborowska E, Wyczalkowska-Tomasik A, Paczek L, Dadlez M, Ufnal M. Chronic, low-dose TMAO treatment reduces diastolic dysfunction and heart fibrosis in hypertensive rats. *Am J Physiol Heart Circ Physiol*. 2018;**315**:H1805-H20.
16. Solanky KS, Bailey NJ, Beckwith-Hall BM, Bingham S, Davis A, Holmes E, Nicholson JK, Cassidy A. Biofluid 1H NMR-based metabonomic techniques in nutrition research - metabolic effects of dietary isoflavones in humans. *J Nutr Biochem*. 2005;**16**:236-44.
17. Barton S, Navarro SL, Buas MF, Schwarz Y, Gu H, Djukovic D, Raftery D, Kratz M, Neuhouser ML, Lampe JW. Targeted plasma metabolome response to variations in dietary glycemic load in a randomized, controlled, crossover feeding trial in healthy adults. *Food Funct*. 2015;**6**:2949-56.
18. Cheung W, Keski-Rahkonen P, Assi N, Ferrari P, Freisling H, Rinaldi S, Slimani N, Zamora-Ros R, Rundle M, Frost G, Gibbons H, Carr E, Brennan L, Cross AJ, Pala V, Panico S, Sacerdote C, Palli D, Tumino R, Kuhn T, Kaaks R, Boeing H, Floegel A, Mancini F, Boutron-Ruault MC, Baglietto L, Trichopoulou A, Naska A, Orfanos P, Scalbert A. A metabolomic study of biomarkers of meat and fish intake. *Am J Clin Nutr*. 2017;**105**:600-8.
19. Bergeron N, Williams PT, Lamendella R, Faghihnia N, Grube A, Li X, Wang Z, Knight R, Jansson JK, Hazen SL, Krauss RM. Diets high in resistant starch increase plasma levels of trimethylamine-N-oxide, a gut microbiome metabolite associated with CVD risk. *Br J Nutr*. 2016;**116**:2020-9.
20. Reeves PG, Nielsen FH, Fahey GC, Jr. AIN-93 purified diets for laboratory rodents: final report of the American Institute of Nutrition ad hoc writing committee on the reformulation of the AIN-76A rodent diet. *J Nutr*. 1993;**123**:1939-51.
21. Koay YC, Wali JA, Luk AWS, Macia L, Cogger VC, Pulpitel TJ, Wahl D, Solon-Biet SM, Holmes A, Simpson SJ, O'Sullivan JF. Ingestion of resistant starch by mice markedly increases microbiome-derived metabolites. *FASEB J*. 2019:fj201900177R.
22. Chen YC, Bui AV, Diesch J, Manasseh R, Hausding C, Rivera J, Haviv I, Agrotis A, Htun NM, Jowett J, Hagemeyer CE, Hannan RD, Bobik A, Peter K. A novel mouse model of atherosclerotic plaque instability for drug testing and mechanistic/therapeutic discoveries using gene and microRNA expression profiling. *Circ Res*. 2013;**113**:252-65.
23. Htun NM, Chen YC, Lim B, Schiller T, Maghzal GJ, Huang AL, Elgass KD, Rivera J, Schneider HG, Wood BR, Stocker R, Peter K. Near-infrared autofluorescence induced by intraplaque hemorrhage and heme degradation as marker for high-risk atherosclerotic plaques. *Nat Commun*. 2017;**8**:75.
24. Wang TJ, Ngo D, Psychogios N, Dejam A, Larson MG, Vasan RS, Ghorbani A, O'Sullivan J, Cheng S, Rhee EP, Sinha S, McCabe E, Fox CS, O'Donnell CJ, Ho JE, Florez JC, Magnusson M, Pierce KA, Souza AL, Yu Y, Carter C, Light PE, Melander O, Clish CB, Gerszten RE. 2-Aminoadipic acid is a biomarker for diabetes risk. *J Clin Invest*. 2013;**123**:4309-17.
25. Kleinert M, Parker BL, Chaudhuri R, Fazakerley DJ, Serup A, Thomas KC, Krycer JR, Sylow L, Fritzen AM, Hoffman NJ. mTORC2 and AMPK differentially regulate muscle triglyceride content via Perilipin 3. *Mol Metab*. 2016;**5**:646-55.
26. R core team. R: A language and environment for statistical computing. *R Foundation for Statistical Computing*. 2018.
27. Callahan BJ, McMurdie PJ, Rosen MJ, Han AW, Johnson AJA, Holmes SP. DADA2: high-resolution sample inference from Illumina amplicon data. *Nat Methods*. 2016;**13**:581.
28. Glöckner FO, Yilmaz P, Quast C, Gerken J, Beccati A, Ciuprina A, Bruns G, Yarza P, Peplies J, Westram R. 25 years of serving the community with ribosomal RNA gene reference databases and tools. *J Biotechnol*. 2017;**261**:169-76.

29. Bodenhofer U, Bonatesta E, Horejš-Kainrath C, Hochreiter S. msa: an R package for multiple sequence alignment. *Bioinformatics*. 2015;**31**:3997-9.
30. Paradis E, Schliep K. ape 5.0: an environment for modern phylogenetics and evolutionary analyses in R. *Bioinformatics*. 2018;**35**:526-8.
31. Lozupone C, Lladser ME, Knights D, Stombaugh J, Knight R. UniFrac: an effective distance metric for microbial community comparison. *ISME J*. 2011;**5**:169.
32. McMurdie PJ, Holmes S. phyloseq: an R package for reproducible interactive analysis and graphics of microbiome census data. *PLoS one*. 2013;**8**:e61217.
33. Wickham H. ggplot2: Elegant Graphics for Data Analysis.: Springer-Verlag New York; 2016.
34. van den Boogaart KG T-DT, Bren M. *Compositions: Compositional data analysis* 2018;**R package v1.**:40-2.
35. Sanchez G, Sanchez MG. Package 'plsdepot'. *Partial Least Squares (PLS) Data Analysis Methods, v 01*. 2012;**17**.
36. Oksanen J, Blanchet FG, Kindt R, Legendre P, Minchin PR, O'hara R, Simpson GL, Solymos P, Stevens MHH, Wagner H. Package 'vegan'. *Community ecology package, version*. 2013;**2**:1-295.
37. Getz GS, Reardon CA. Do the Apoe-/- and Ldlr-/- Mice Yield the Same Insight on Atherogenesis? *Arterioscler Thromb Vasc Biol*. 2016;**36**:1734-41.
38. Cartland SP, Genner SW, Martinez GJ, Robertson S, Kockx M, Lin RC, O'Sullivan JF, Koay YC, Manuneedhi Cholan P, Kebede MA, Murphy AJ, Masters S, Bennett MR, Jessup W, Kritharides L, Geczy C, Patel S, Kavurma MM. TRAIL-Expressing Monocyte/Macrophages Are Critical for Reducing Inflammation and Atherosclerosis. *iScience*. 2019;**12**:41-52.
39. Zhang A, Mitchell S, Smith R. Dietary precursors of trimethylamine in man: a pilot study. *Food Chem Toxicol*. 1999;**37**:515-20.
40. Stefanadis C, Antoniou CK, Tsiachris D, Pietri P. Coronary Atherosclerotic Vulnerable Plaque: Current Perspectives. *J Am Heart Assoc*. 2017;**6**.
41. Gkaliagkousi E, Passacquale G, Douma S, Zamboulis C, Ferro A. Platelet Activation in Essential Hypertension: Implications for Antiplatelet Treatment. *Am J Hypertens*. 2010;**23**:229-36.
42. de Meirelles LR, Mendes-Ribeiro AC, Santoro MM, Mendes MA, da Silva MN, Mann GE, Brunini TM. Inhibitory effects of endogenous L-arginine analogues on nitric oxide synthesis in platelets: role in platelet hyperaggregability in hypertension. *Clin Exp Pharmacol Physiol*. 2007;**34**:1267-71.
43. Bennett BJ, de Aguiar Vallim TQ, Wang Z, Shih DM, Meng Y, Gregory J, Allayee H, Lee R, Graham M, Crooke R, Edwards PA, Hazen SL, Lusis AJ. Trimethylamine-N-oxide, a metabolite associated with atherosclerosis, exhibits complex genetic and dietary regulation. *Cell Metab*. 2013;**17**:49-60.
44. Lindskog Jonsson A, Caesar R, Akrami R, Reinhardt C, Fak Hallenius F, Boren J, Backhed F. Impact of Gut Microbiota and Diet on the Development of Atherosclerosis in Apoe(-/-) Mice. *Arterioscler Thromb Vasc Biol*. 2018;**38**:2318-26.
45. Kurilshikov A, van den Munckhof ICL, Chen L, Bonder MJ, Schraa K, Rutten JHW, Riksen NP, de Graaf J, Oosting M, Sanna S, Joosten LAB, van der Graaf M, Brand T, Koonen DPY, van Faassen M, LifeLines Deep Cohort Study BMC, Slagboom PE, Xavier RJ, Kuipers F, Hofker MH, Wijmenga C, Netea MG, Zhernakova A, Fu J. Gut Microbial Associations to Plasma Metabolites Linked to Cardiovascular Phenotypes and Risk. *Circ Res*. 2019;**124**:1808-20.
46. Michel JB, Virmani R, Arbustini E, Pasterkamp G. Intraplaque haemorrhages as the trigger of plaque vulnerability. *Eur Heart J*. 2011;**32**:1977-85, 85a, 85b, 85c.

47. Jameson E, Doxey AC, Airs R, Purdy KJ, Murrell JC, Chen Y. Metagenomic data-mining reveals contrasting microbial populations responsible for trimethylamine formation in human gut and marine ecosystems. *Microbial genomics*. 2016;**2**.
48. Motika MS, Zhang J, Zheng X, Riedler K, Cashman JR. Novel variants of the human flavin-containing monooxygenase 3 (FMO3) gene associated with trimethylaminuria. *Mol Genet Metab Rep*. 2009;**97**:128-35.
49. Chen Y, Patel NA, Crombie A, Scrivens JH, Murrell JC. Bacterial flavin-containing monooxygenase is trimethylamine monooxygenase. *Proc Natl Acad Sci USA*. 2011;**108**:17791-6.
50. Janeiro MH, Ramirez MJ, Milagro FI, Martinez JA, Solas M. Implication of Trimethylamine N-Oxide (TMAO) in Disease: Potential Biomarker or New Therapeutic Target. *Nutrients*. 2018;**10**.
51. Clavel T, Charrier C, Braune A, Wenning M, Blaut M, Haller D. Isolation of bacteria from the ileal mucosa of TNFdeltaARE mice and description of Enterorhabdus mucosicola gen. nov., sp. nov. *Int J Syst Evol Microbiol*. 2009;**59**:1805-12.
52. Ye J, Lee JW, Presley LL, Bent E, Wei B, Braun J, Schiller NL, Straus DS, Borneman J. Bacteria and bacterial rRNA genes associated with the development of colitis in IL-10−/− mice. *Inflamm Bowel Dis*. 2008;**14**:1041-50.
53. Benson AK, Kelly SA, Legge R, Ma F, Low SJ, Kim J, Zhang M, Oh PL, Nehrenberg D, Hua K, Kachman SD, Moriyama EN, Walter J, Peterson DA, Pomp D. Individuality in gut microbiota composition is a complex polygenic trait shaped by multiple environmental and host genetic factors. *PNAS*. 2010;**107**:18933-8.
54. Knights D, Lassen KG, Xavier RJ. Advances in inflammatory bowel disease pathogenesis: linking host genetics and the microbiome. *Gut*. 2013;**62**:1505-10.
55. Thaiss CA, Levy M, Korem T, Dohnalova L, Shapiro H, Jaitin DA, David E, Winter DR, Gury-BenAri M, Tatirovsky E, Tuganbaev T, Federici S, Zmora N, Zeevi D, Dori-Bachash M, Pevsner-Fischer M, Kartvelishvily E, Brandis A, Harmelin A, Shibolet O, Halpern Z, Honda K, Amit I, Segal E, Elinav E. Microbiota Diurnal Rhythmicity Programs Host Transcriptome Oscillations. *Cell*. 2016;**167**:1495-510 e12.
56. Balagam B, Richardson DE. The mechanism of carbon dioxide catalysis in the hydrogen peroxide N-oxidation of amines. *Inorg Chem*. 2008;**47**:1173-8.
57. Schöneich C. Methionine oxidation by reactive oxygen species: reaction mechanisms and relevance to Alzheimer's disease. *Biochim Biophys Acta (BBA) - Proteins and Proteomics*. 2005;**1703**:111-9.
58. Ashfaq S, Abramson JL, Jones DP, Rhodes SD, Weintraub WS, Hooper WC, Vaccarino V, Harrison DG, Quyyumi AA. The Relationship Between Plasma Levels of Oxidized and Reduced Thiols and Early Atherosclerosis in Healthy Adults. *J Am Coll Cardiol*. 2006;**47**:1005-11.
59. Fuentes-Zaragoza E, Riquelme-Navarrete MJ, Sánchez-Zapata E, Pérez-Álvarez JA. Resistant starch as functional ingredient: A review. *Food Res Int*. 2010;**43**:931-42.
60. Chiang JY. Bile acids: regulation of synthesis. *J Lipid Res*. 2009;**50**:1955-66.
61. Myant N, Mitropoulos K. Cholesterol 7 alpha-hydroxylase. *J Lipid Res*. 1977;**18**:135-53.
62. Andersson KE, Axling U, Xu J, Sward K, Ahrne S, Molin G, Holm C, Hellstrand P. Diverse effects of oats on cholesterol metabolism in C57BL/6 mice correlate with expression of hepatic bile acid-producing enzymes. *Eur J Nutr*. 2013;**52**:1755-69.
63. Gremmel T, Perkmann T, Kopp CW, Seidinger D, Eichelberger B, Koppensteiner R, Steiner S, Panzer S. Interleukin-6 and asymmetric dimethylarginine are associated with platelet activation after percutaneous angioplasty with stent implantation. *PLoS One*. 2015;**10**:e0122586.

64. Ferroni P, Guagnano MT, Falco A, Paoletti V, Manigrasso MR, Michetti N, Santilli F, Guadagni F, Basili S, Davi G. Association of low-grade inflammation and platelet activation in patients with hypertension with microalbuminuria. *Clin Sci (Lond)*. 2008;**114**:449-55.
65. Gkaliagkousi E, Ritter J, Ferro A. Platelet-derived nitric oxide signaling and regulation. *Circ Res*. 2007;**101**:654-62.
66. Li XS, Obeid S, Klingenberg R, Gencer B, Mach F, Raber L, Windecker S, Rodondi N, Nanchen D, Muller O, Miranda MX, Matter CM, Wu Y, Li L, Wang Z, Alamri HS, Gogonea V, Chung YM, Tang WH, Hazen SL, Luscher TF. Gut microbiota-dependent trimethylamine N-oxide in acute coronary syndromes: a prognostic marker for incident cardiovascular events beyond traditional risk factors. *Eur Heart J*. 2017;**38**:814-24.
67. Chen YC, Rivera J, Peter K. Tandem Stenosis to Induce Atherosclerotic Plaque Instability in the Mouse. *Methods Mol Biol*. 2015;**1339**:333-8.
68. Rashid I, Maghzal GJ, Chen YC, Cheng D, Talib J, Newington D, Ren M, Vajandar SK, Searle A, Maluenda A, Lindstedt EL, Jabbour A, Kettle AJ, Bongers A, Power C, Michaelsson E, Peter K, Stocker R. Myeloperoxidase is a potential molecular imaging and therapeutic target for the identification and stabilization of high-risk atherosclerotic plaque. *Eur Heart J*. 2018;**39**:3301-10.
69. Diehl P, Nienaber F, Zaldivia MTK, Stamm J, Siegel PM, Mellett NA, Wessinger M, Wang X, McFadyen JD, Bassler N, Puetz G, Htun NM, Braig D, Habersberger J, Helbing T, Eisenhardt SU, Fuller M, Bode C, Meikle PJ, Chen YC, Peter K. Lysophosphatidylcholine is a Major Component of Platelet Microvesicles Promoting Platelet Activation and Reporting Atherosclerotic Plaque Instability. *Thromb Haemost*. 2019;**119**:1295-310.
70. Tan Y, Zhou J, Liu C, Zhou P, Sheng Z, Li J, Chen R, Song L, Zhao H, Xu B. Association between plasma trimethylamine N-oxide and neoatherosclerosis in patients with very late stent thrombosis. *Can J Cardiol*. 2019.
71. Liu X, Xie Z, Sun M, Wang X, Li J, Cui J, Zhang F, Yin L, Huang D, Hou J, Tian J, Yu B. Plasma trimethylamine N-oxide is associated with vulnerable plaque characteristics in CAD patients as assessed by optical coherence tomography. *Int J Cardiol*. 2018;**265**:18-23.
72. Fu Q, Zhao M, Wang D, Hu H, Guo C, Chen W, Li Q, Zheng L, Chen B. Coronary plaque characterization assessed by optical coherence tomography and plasma trimethylamine-N-oxide levels in patients with coronary artery disease. *Am J Cardiol*. 2016;**118**:1311-5.
73. Zeller M, Korandji C, Guilland JC, Sicard P, Vergely C, Lorgis L, Beer JC, Duvillard L, Lagrost AC, Moreau D, Gambert P, Cottin Y, Rochette L. Impact of asymmetric dimethylarginine on mortality after acute myocardial infarction. *Arterioscler Thromb Vasc Biol*. 2008;**28**:954-60.
74. Cavusoglu E, Ruwende C, Chopra V, Yanamadala S, Eng C, Pinsky DJ, Marmur JD. Relationship of baseline plasma ADMA levels to cardiovascular outcomes at 2 years in men with acute coronary syndrome referred for coronary angiography. *Coron Artery Dis*. 2009;**20**:112-7.

## FIGURE LEGENDS

**Figure 1. Plasma metabolites and hepatic FMOs expression in low choline (LC) vs high choline (HC)-fed mice.** Normalized abundance of (A) choline, betaine, and carnitine; (B) TMA and TMAO; (C) CA and DCA in $ApoE^{-/-}$ and $Ldlr^{-/-}$ mice. Data are expressed as mean ± SEM and are representative of two independent experiments (n = 12 mice/diet for $ApoE^{-/-}$; n = 9 mice/low choline, n = 12 mice/high choline diet ($Ldlr^{-/-}$). (D) Relative liver mRNA of FMO1, FMO3 and FMO5 from $Ldlr^{-/-}$ mice (n = 12 /diet). Data are from a single representative experiment. All data were analysed using Student's t-test. *p < 0.05, **p < 0.01, ***p < 0.001, ****p < 0.0001. TMA = trimethylamine, TMAO = trimethylamine-N-oxide, CA = cholic acid, DCA = deoxycholic acid, FMO = flavin-containing monooxygenase.

**Figure 2. Plasma and faecal metabolites, and hepatic gene expression in resistant starch- (RS) *vs* native starch- (NS) mice.** Normalized abundance of plasma and faecal levels of (A, B) TMA and TMAO; (C,D) choline, betaine, and carnitine; (E,F) CA and DCA. Data are shown as mean ± SEM and are representative of two independent experiments with n = 6 /diet. Relative liver mRNA of (G) HMGCR and CYP7A1, (H) FXR, FMO1, FMO2 and FMO3 in the liver of NS- and RS-fed mice (mean ± SEM, data are from a single representative experiment with n = 6 /NS diet, n = 7 /RS diet). All data were analysed using Student's t-test. *p < 0.05, **p < 0.01, ***p < 0.001, ****p < 0.0001. HMGCR = 3-hydroxy-3-methylglutaryl-coenzyme A reductase, CYP7A1 = cholesterol 7α-hydroxylase, and FXR = farnesoid X receptor.

**Figure 3. Correlations of the bacterial gut microbiome with metabolites that exhibit major changes upon dietary interventions.** Principal coordinate analysis ordination of weighted UniFrac distances between (A) HC-fed or LC-fed $ApoE^{-/-}$ mice (n = 12 mice/diet),

(C) RS-fed (n = 4) or NS-fed (n = 5) C57BL/6J mice. Ellipses represent 95% confidence intervals, and analysis of variance indicates significant difference between (A) HC vs LC diets (P = 0.002) and (C) RS vs NS diets (P = 0.009). Partial least squares correlations between metabolite and amplicon sequence variant (ASV) abundance in (B) HC-fed or LC-fed ApoE$^{-/-}$ mice (n = 12/diet), and (D) RS-fed (n = 4) or NS-fed (n = 5) C57BL/6J mice.

**Figure 4**. **Histological atherosclerotic plaque characteristics in LC vs HC diet.** Data plots showing (A, F) atherosclerotic plaque burden, (B, G) necrotic core size, (C, H) neutral lipid, (D, I) foam cell composition, and (E, J) collagen content in both strains of mice (n ≥ 8 per group). Shown are representative histological images of the different analysis for LC and HC diets in ApoE$^{-/-}$ mice. Data shown are representative of three independent experiments and all data are presented as median and interquartile range. Statistical analysis was performed using non-parametric Mann-Whitney test.

**Figure 5. Lipids, inflammatory cell count, platelet activation, and plasma levels of ADMA and L-NMMA in LC vs HC.** Data plots show (A) triglycerides, (B) total cholesterol, (C) HDL, (D) LDL, (E) circulating lymphocytes, (F) monocytes, (G) neutrophils (E to G: Sysmex data), (H) platelet activation (as indicated by surface expression of platelet P-selectin in flow cytometry) in ApoE$^{-/-}$mice (n = 9-13 per group). Data are presented as median and interquartile range and statistical analysis was performed using non-parametric Mann-Whitney tests. (I) plasma ADMA and L-NMMA. mean ± SEM of n = 11-12 per group. Metabolomic data were analysed using Student's t-test and data shown are representative of a single experiment. *p < 0.05, **p < 0.01, ****p < 0.0001. HDL = high-density lipoprotein, LDL = low-density lipoprotein, ADMA = asymmetric dimethylarginine, L-NMMA = $N^G$-monomethyl-L-arginine.

**Figure 6. Unstable plaque histology in tandem-stenosis model on LC vs HC.** Box-plots indicate (A) neutral lipids by oil red O staining, (B) CD68, (C) VCAM-1, (D) SMA, (E) platelet content by CD42c marker, (F) collagen, (G) iron deposition by Perl's iron staining, and (H) erythrocyte marker TER-119 in $ApoE^{-/-}$mice (n = 8-12 per group). *p < 0.05, **p < 0.01. CD68 = cluster of differentiation 68, VCAM = vascular cell adhesion protein 1, SMA = smooth muscle actin. Representative images showing Perl's and Ter-119 staining in LC and HC diets. Data shown are representative of three independent experiments and all data are presented as median and interquartile range. Statistical analysis was performed using non-parametric Mann-Whitney test.

**Figure 7. No association of plasma TMAO with coronary artery calcium score and carotid IMT in the Framingham Heart Study Offspring cohort, stratified to age tertiles.** (A) comparison of plasma TMAO levels and coronary artery calcium score (CAS) in 628 individuals, and (B) plasma TMAO levels and carotid intima-media thickness (IMT) in 587 individuals. TMAO = trimethylamine-N-oxide, CAS = coronary artery calcium score, IMT = intima-media thickness. Line represents linear regression and *p* values were calculated from t statistics and are illustrated in each plot.

**Graphical Abstract**

A schema summarising the proposed differential routes of TMAO generation. On high-choline diets, microbiota *lachnoclostriudium* and *entororhabdus* generate a pro-oxidative milieu in the gut, leading to oxidation of TMA to TMAO, which is then absorbed into the circulation. On high-fibre diets, *bacteroidales* and *allobaculum* are predominant, and there is increased concentrations of bile acids that activate FMOs that convert TMA to TMAO in the liver, which then enters the circulation.

## FIGURES

### Figure 1.

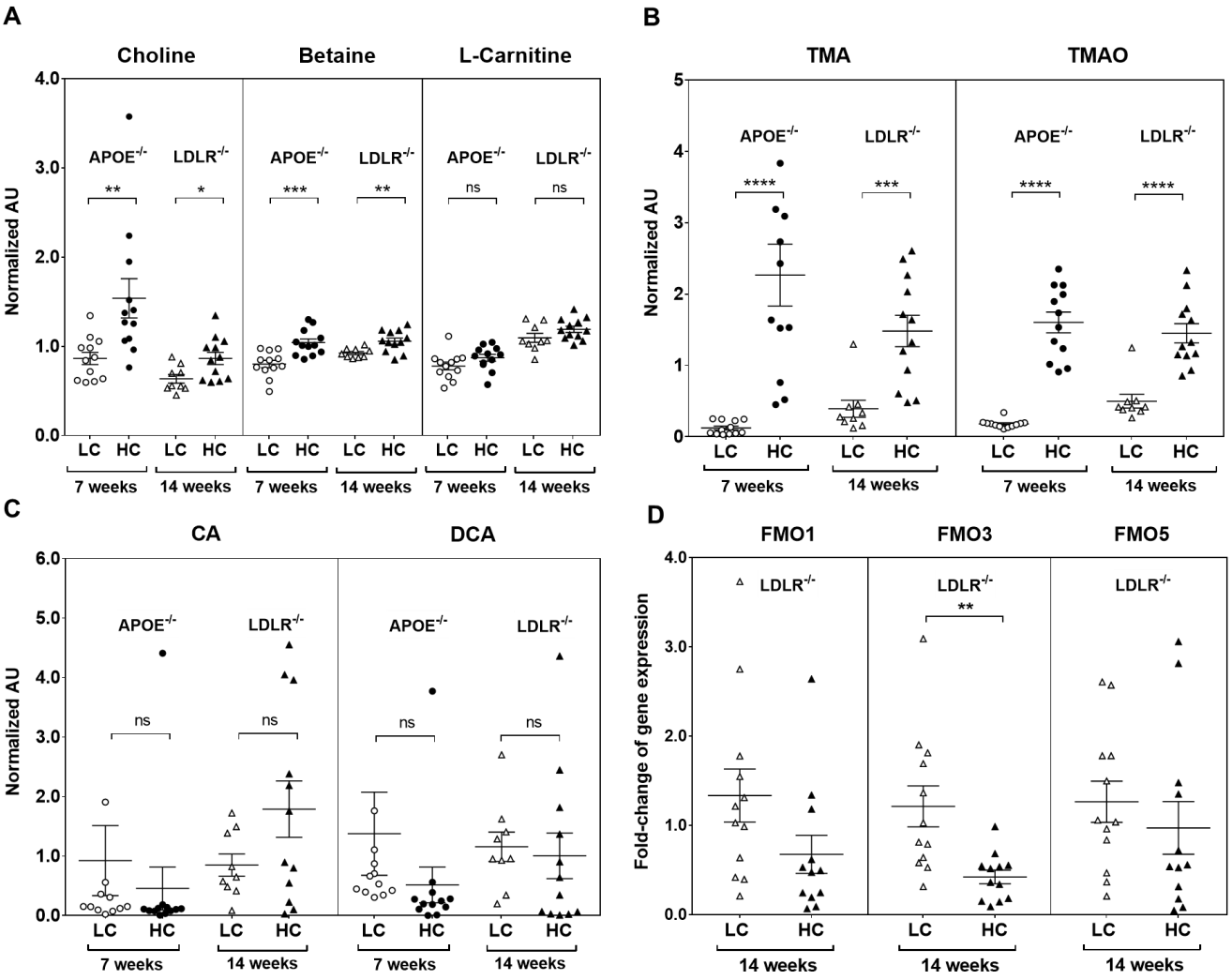

**Figure 2.**

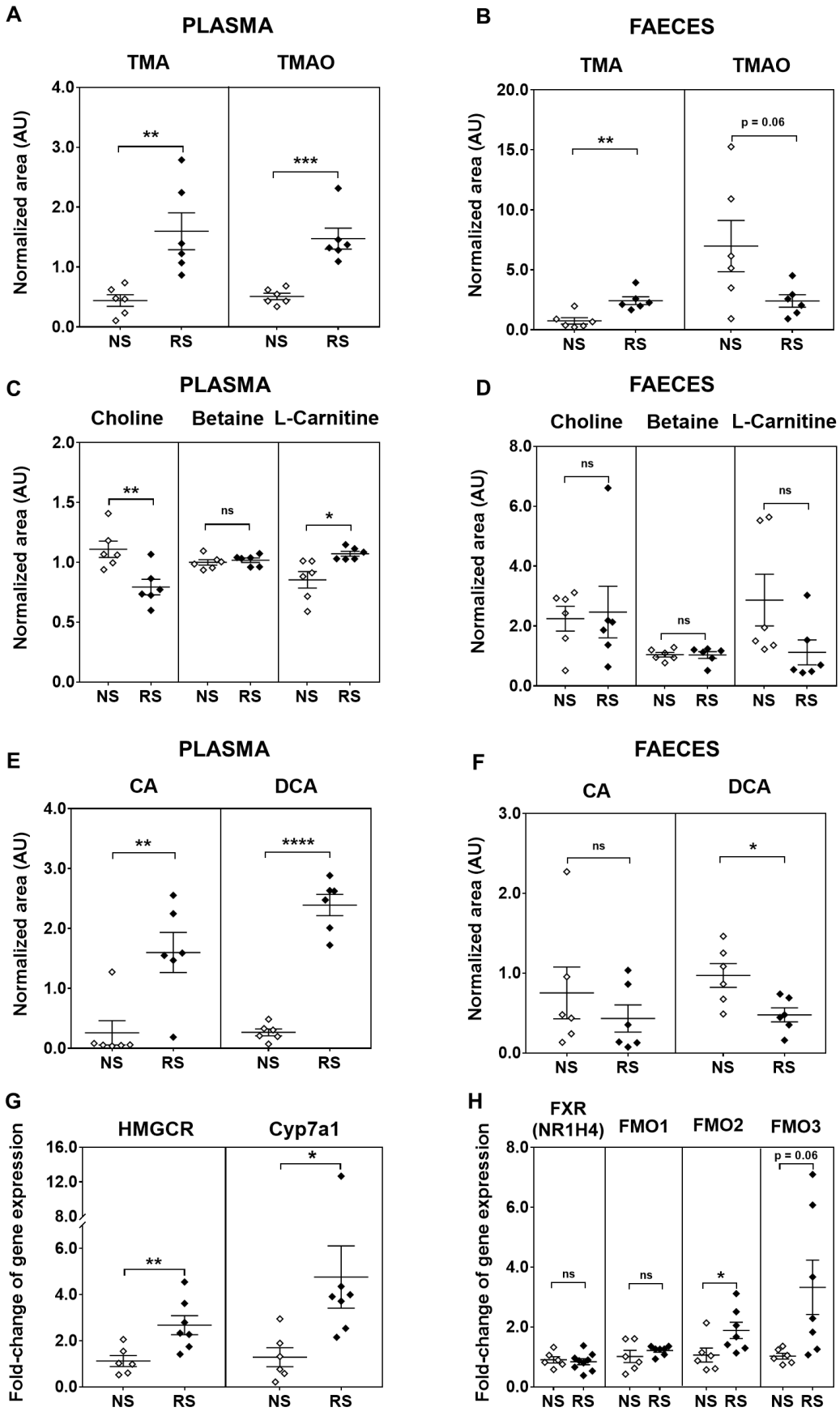

**Figure 3.**

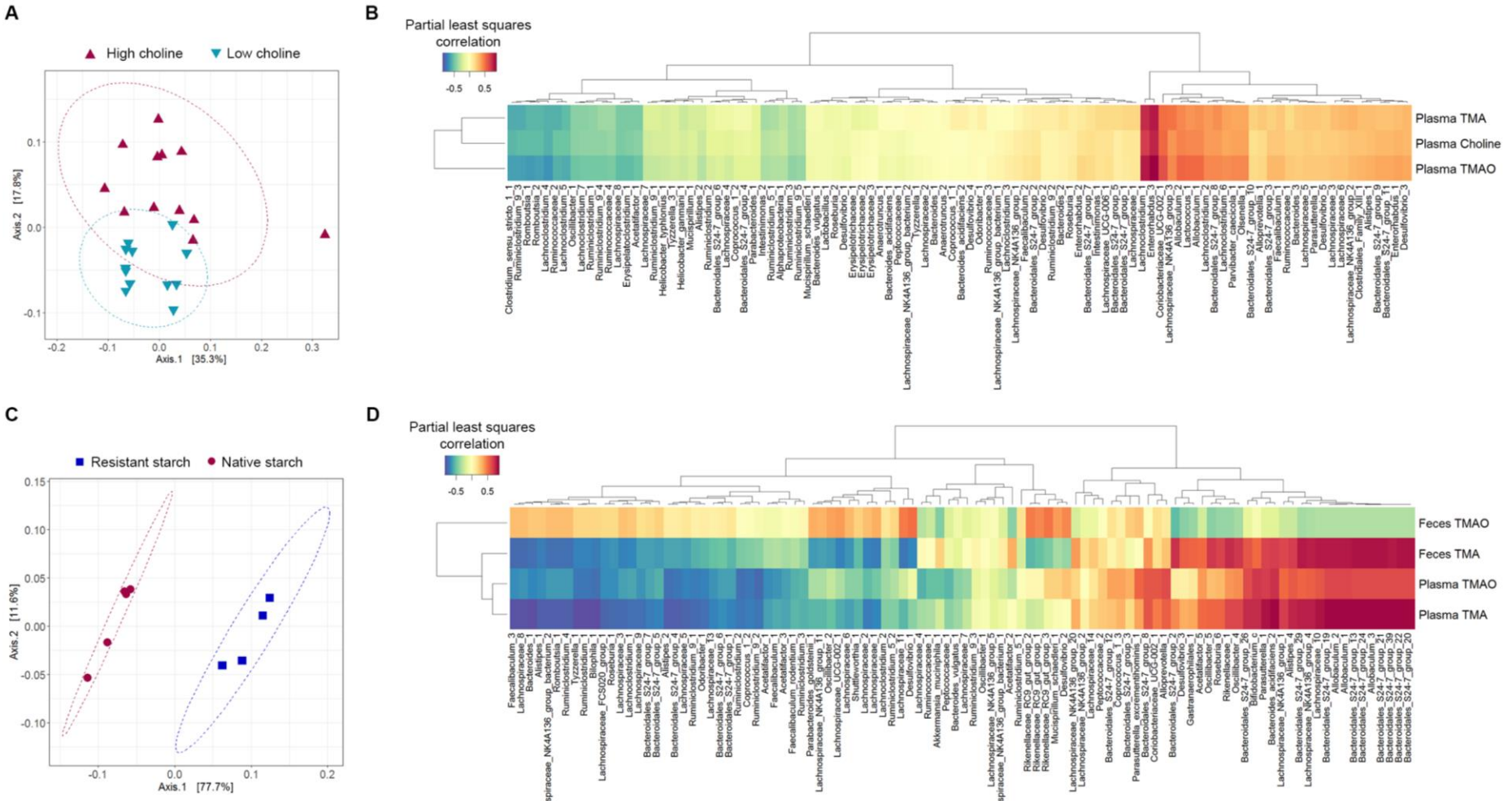

**Figure 4.**

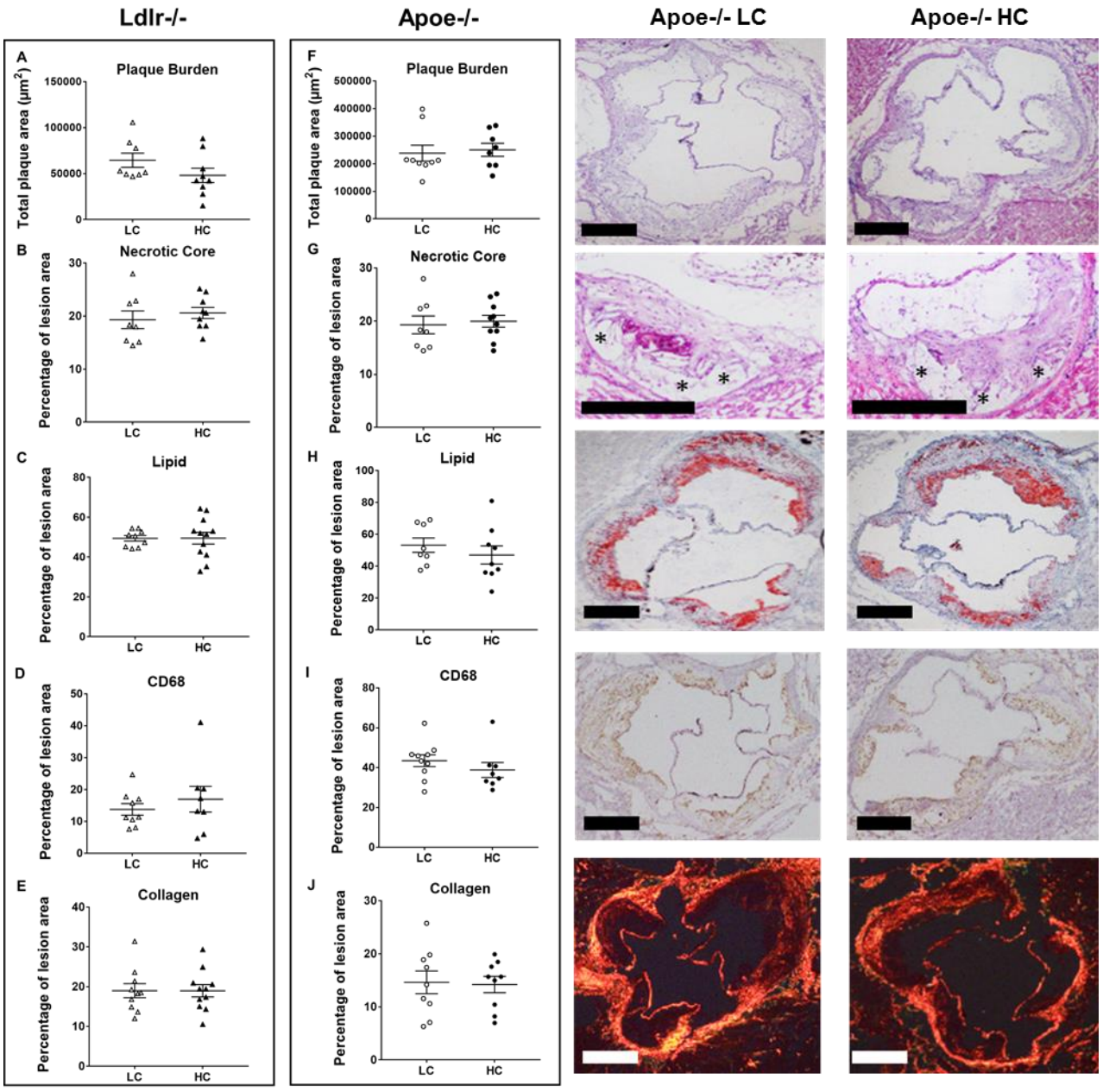

**Figure 5.**

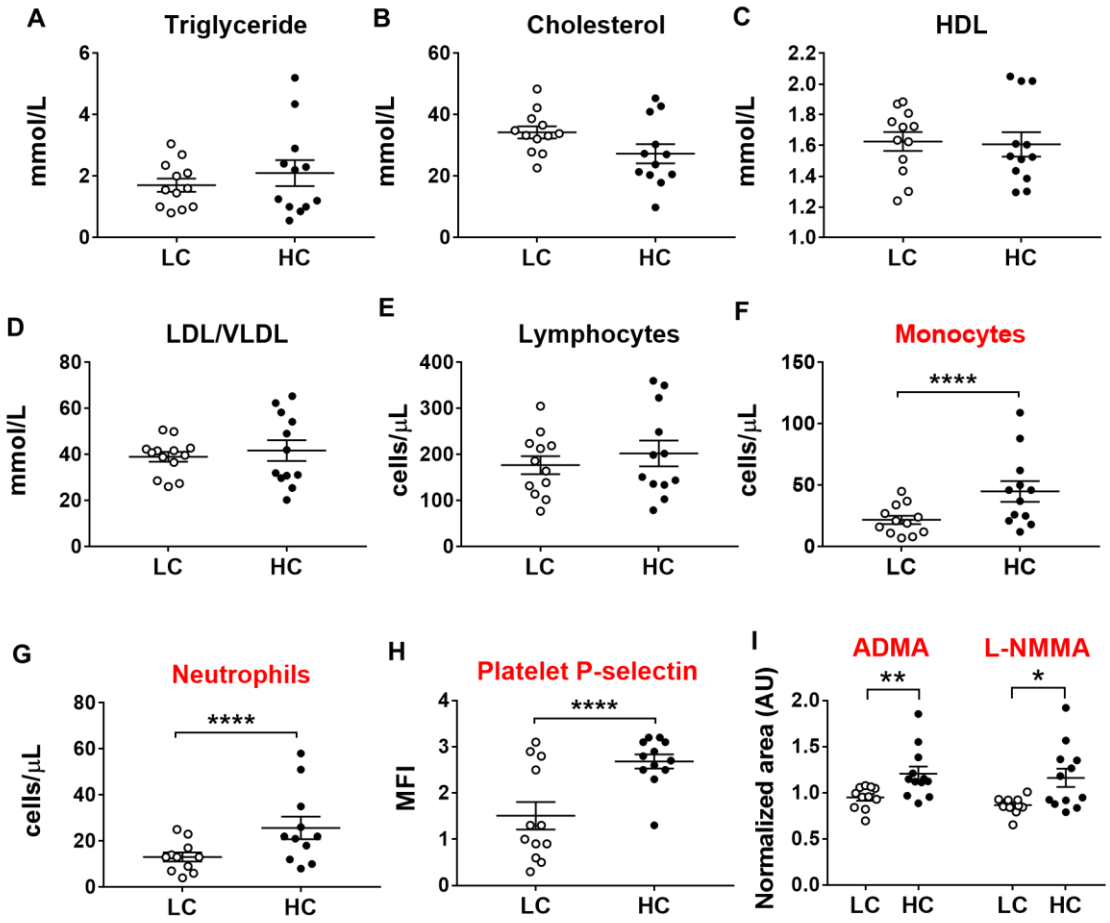

**Figure 6.**

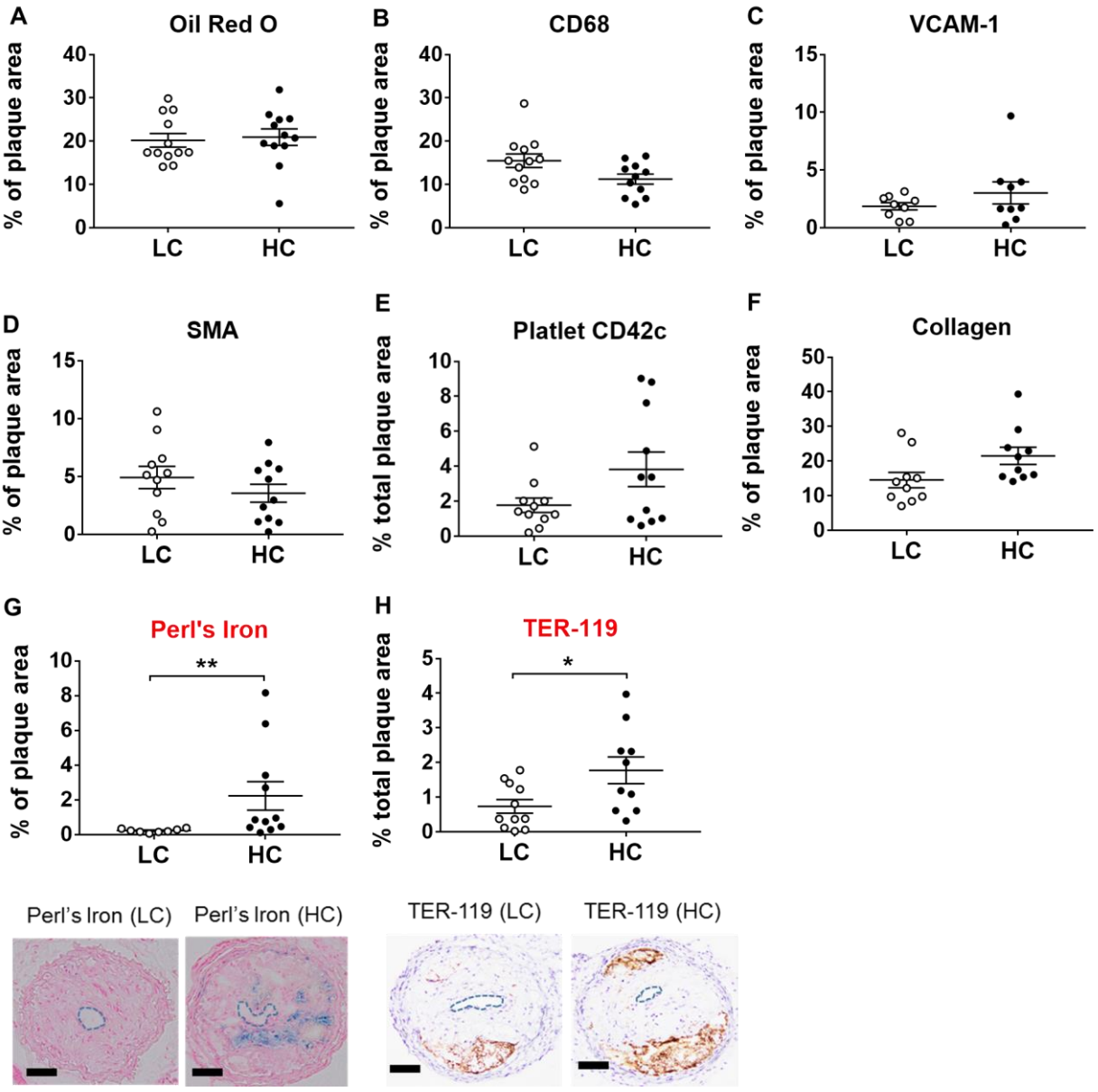

**Figure 7.**

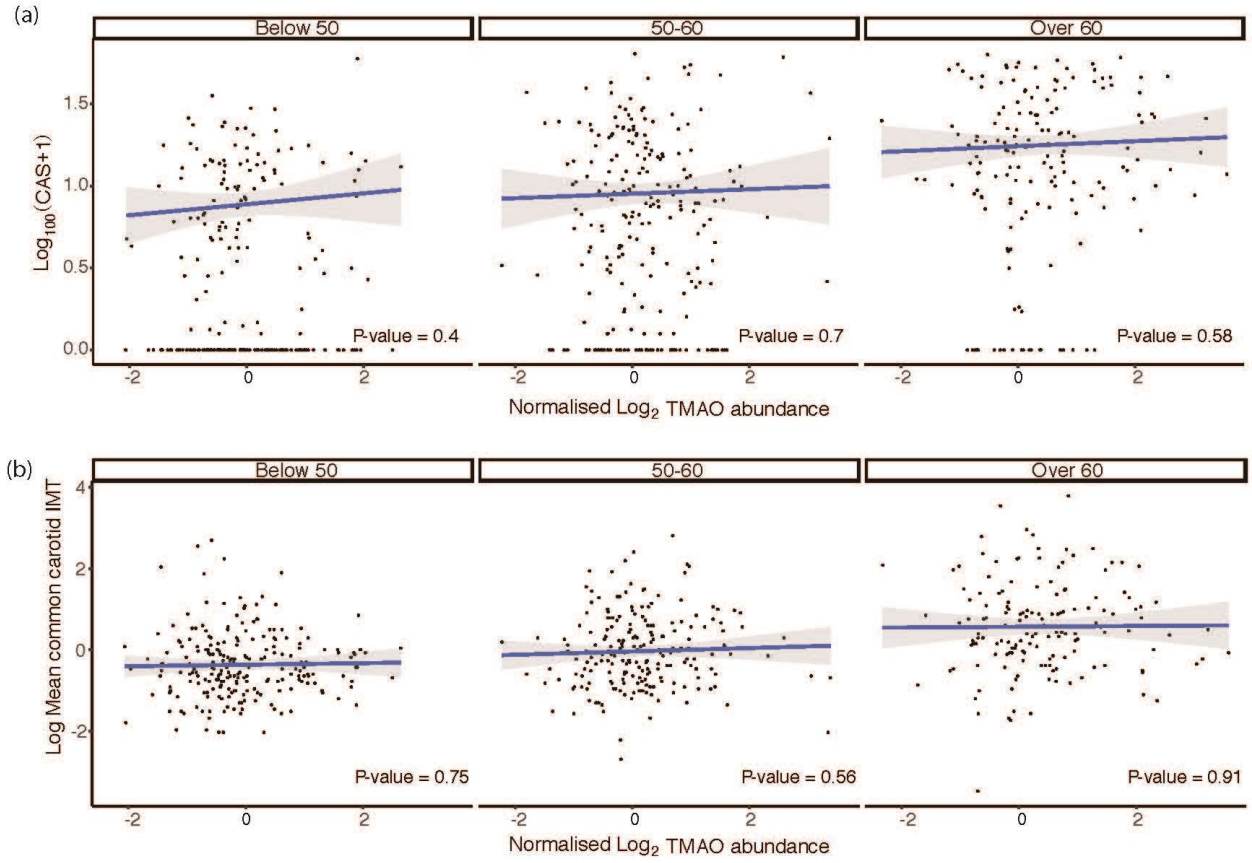

## Graphical Abstract

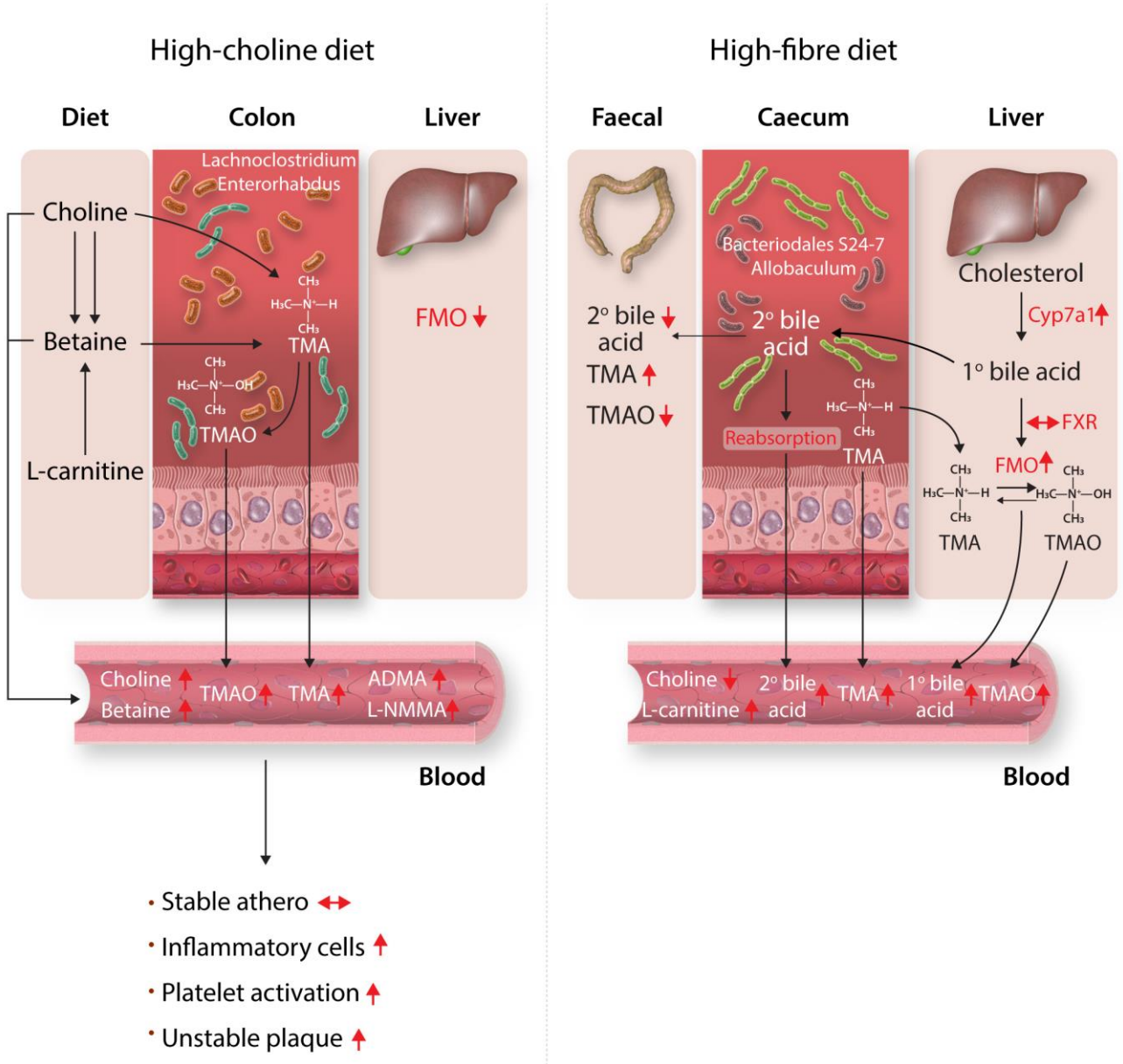

Figure 1

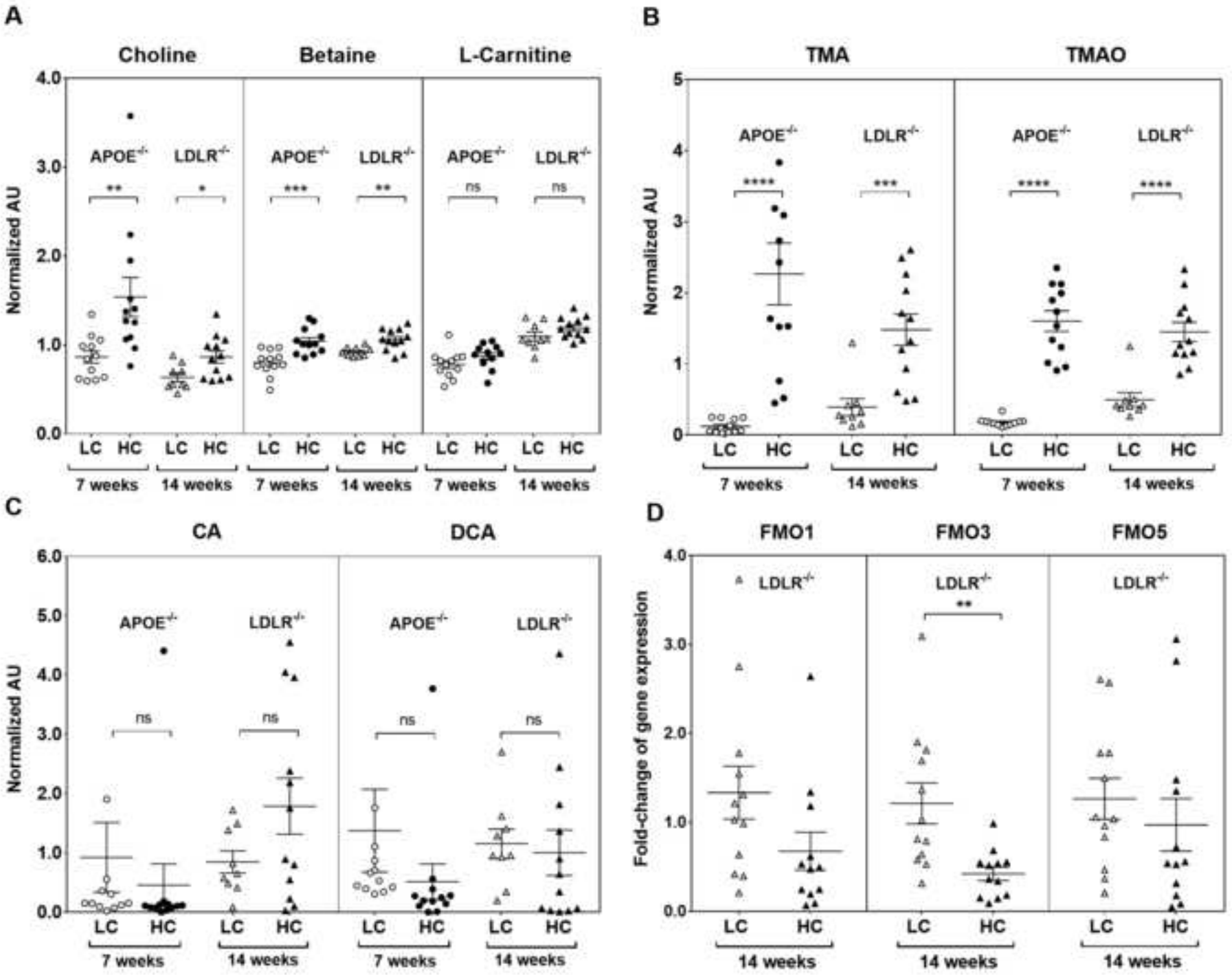

Figure 2



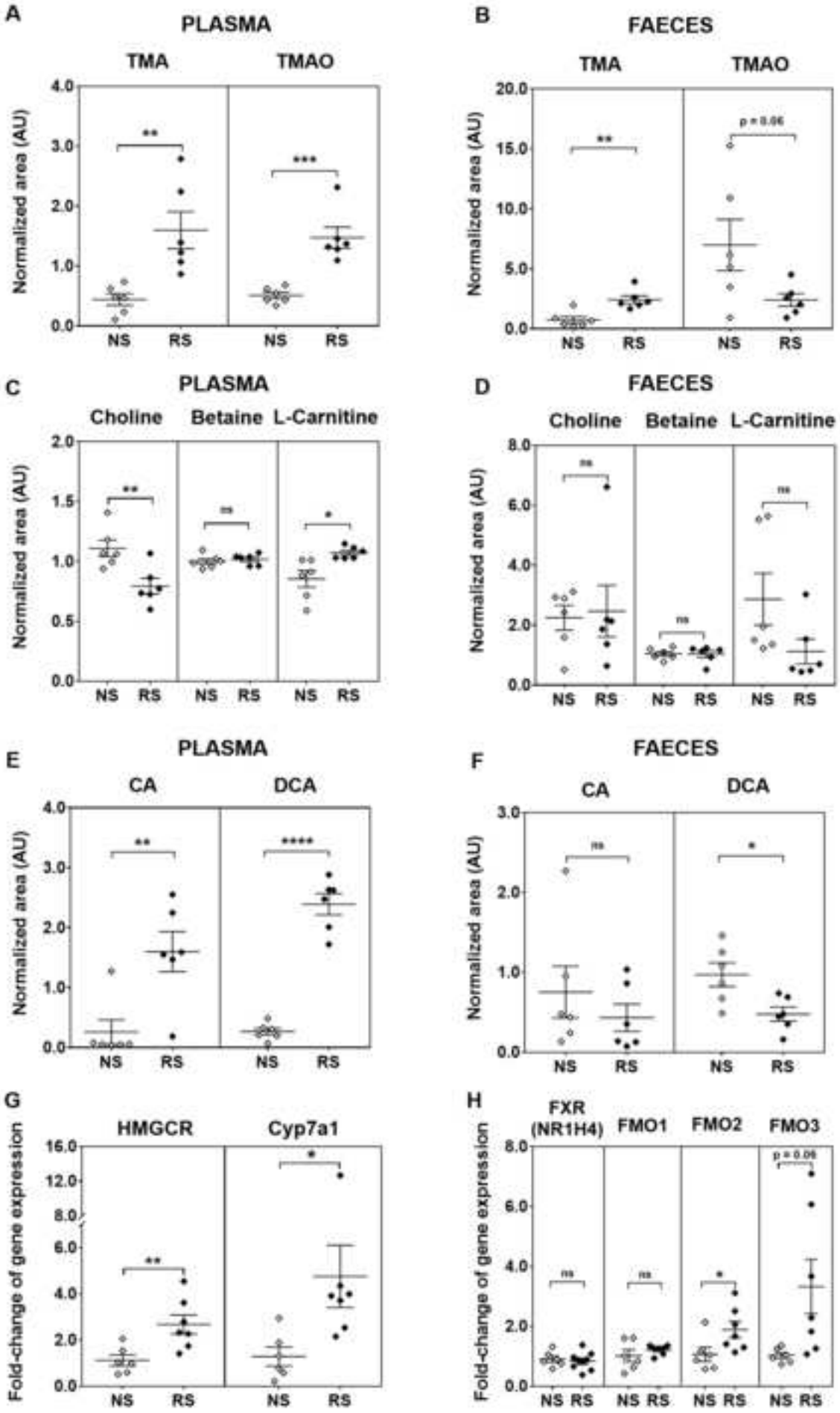

Figure 3

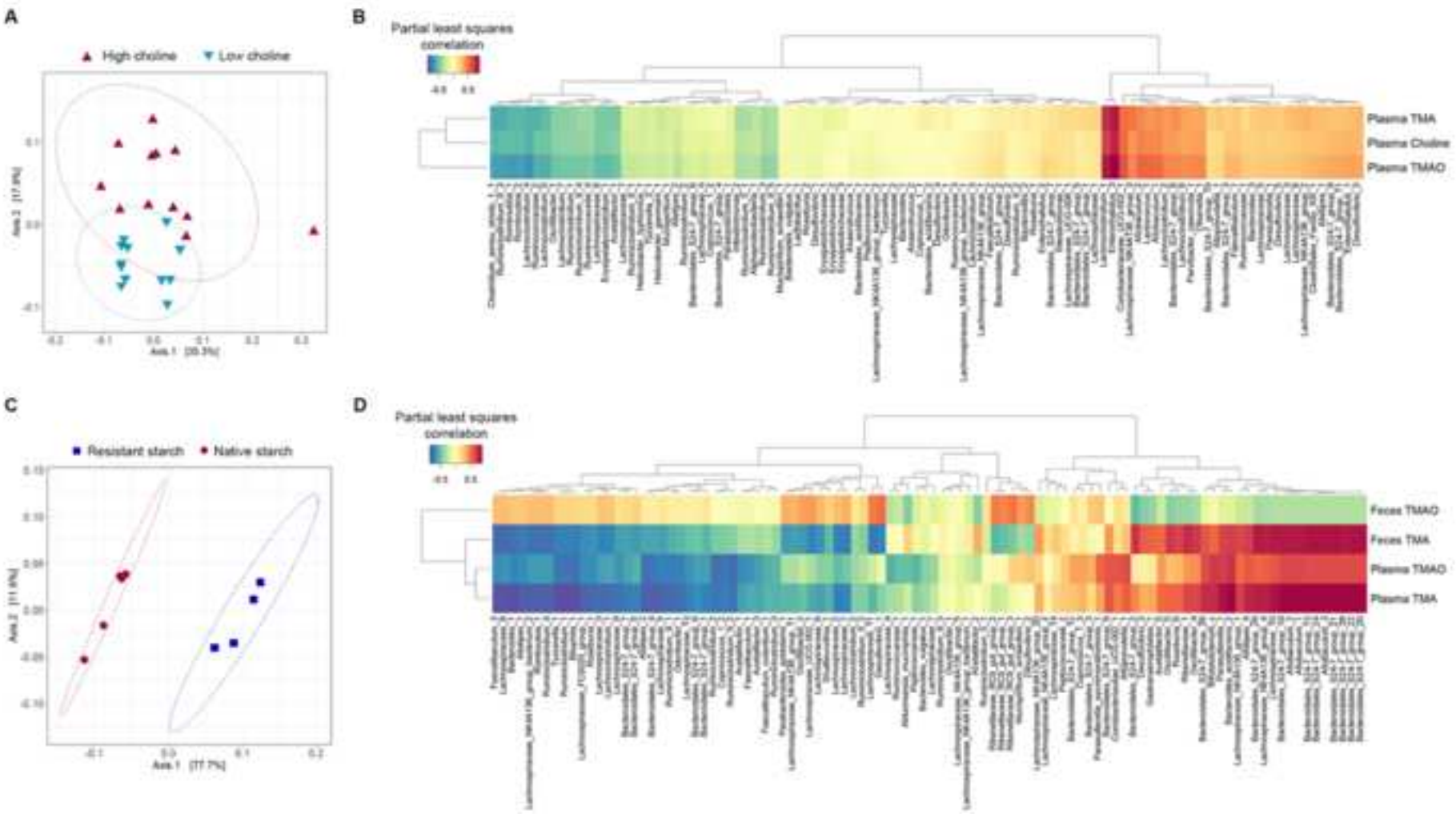

Figure 4

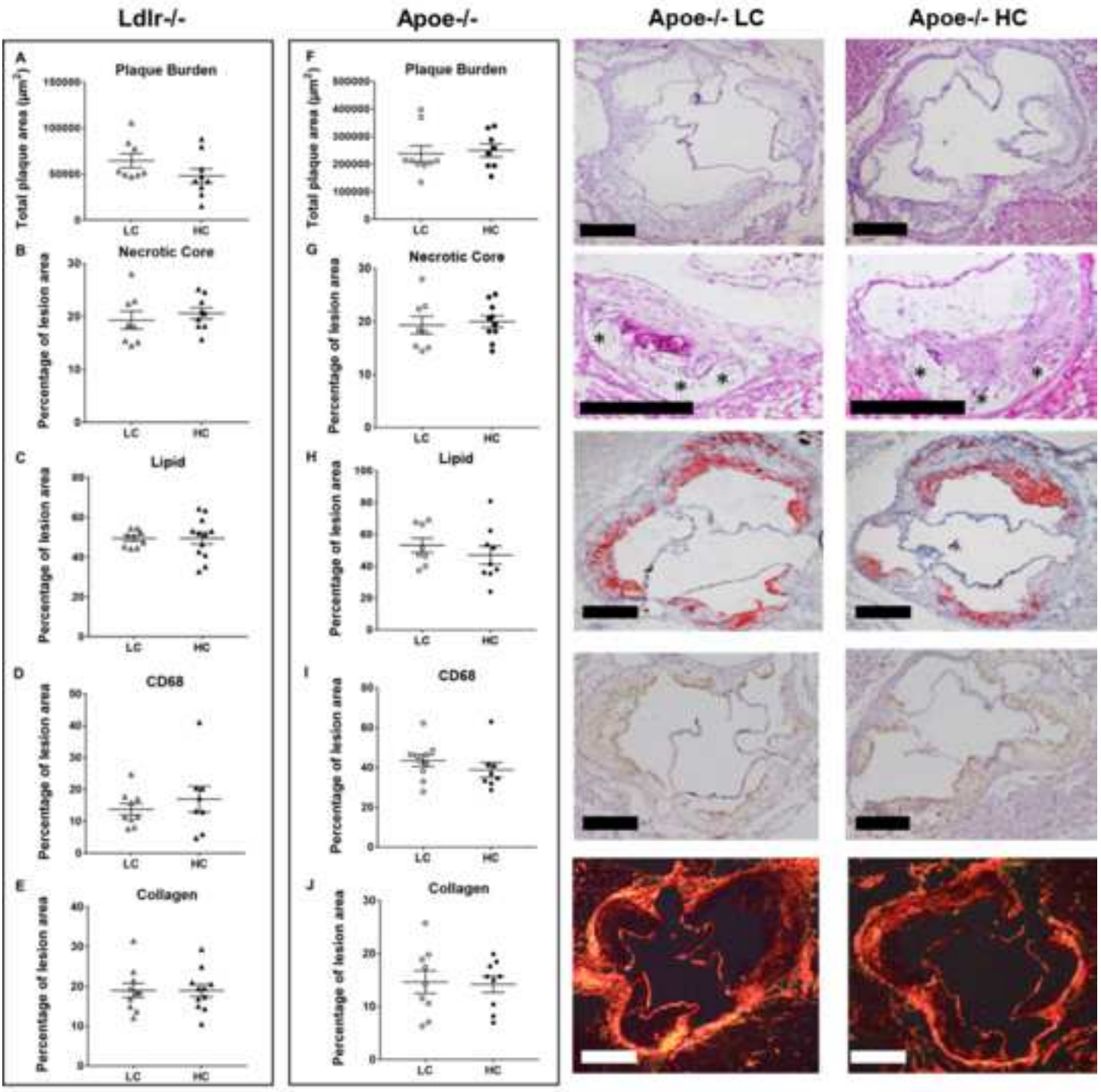

Figure 5

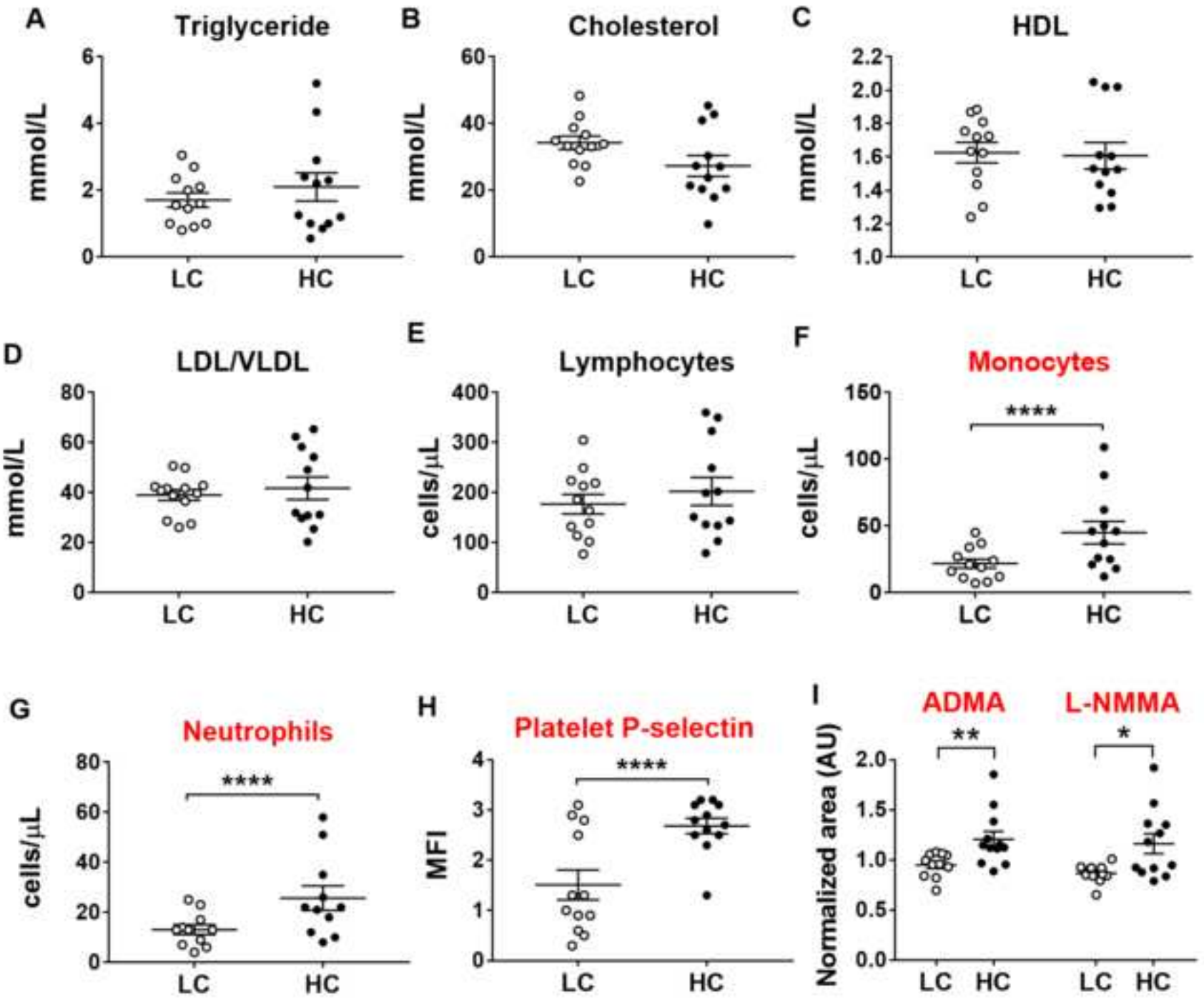

Figure 6

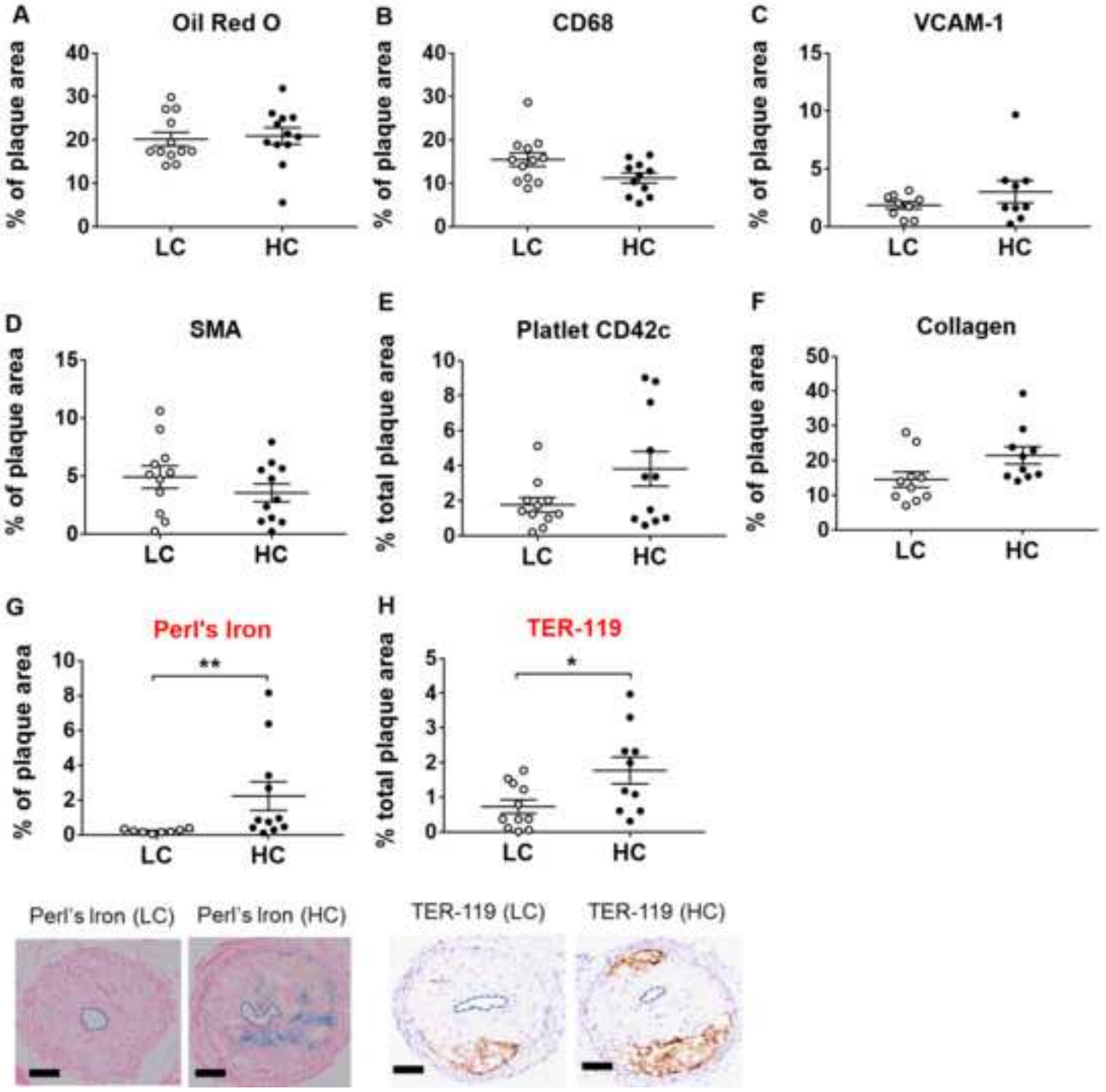

Figure 7

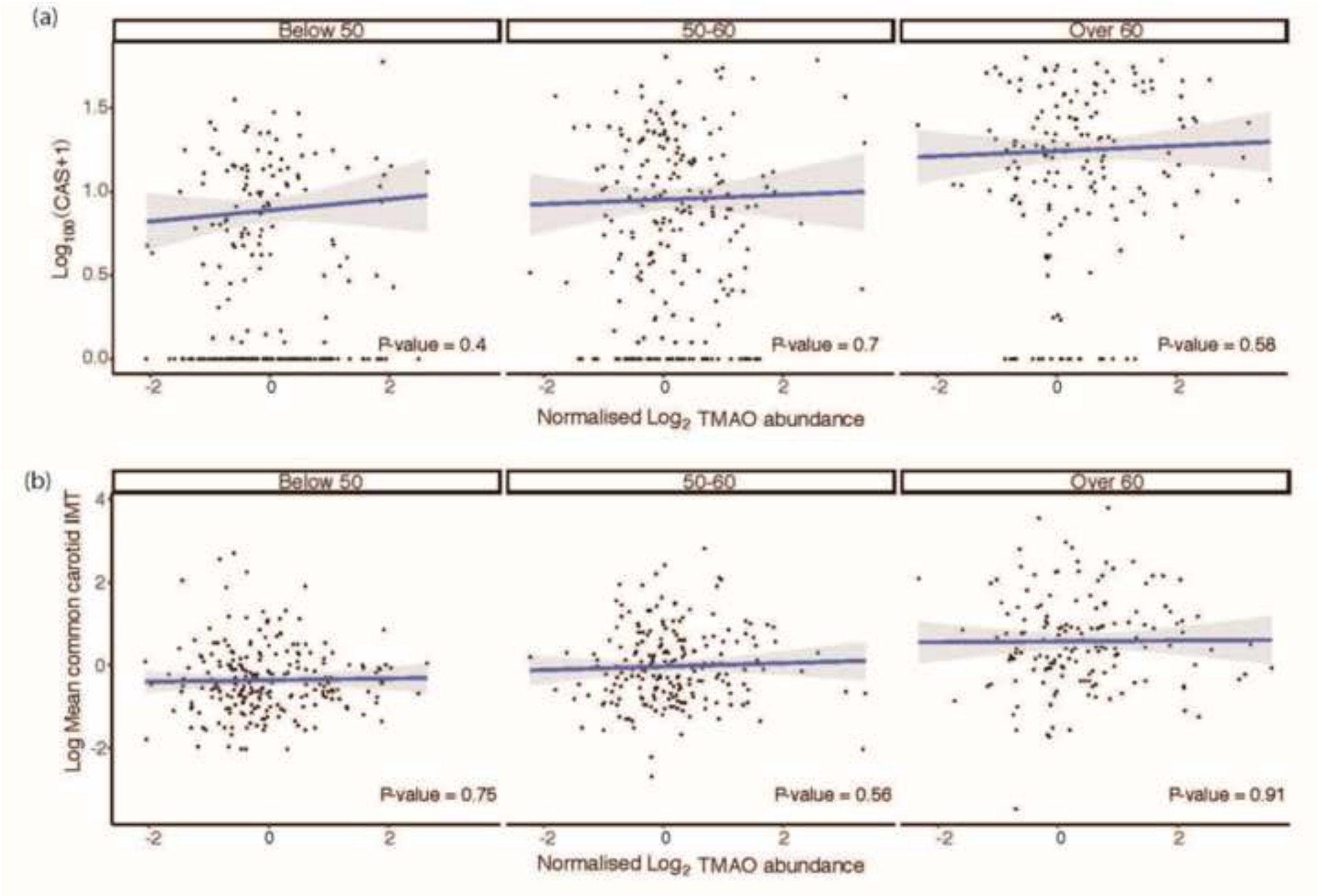

Graphical abstract